NASA CR-774

IMPROVED ION SOURCES

Prepared under Contract No. NAS 5-3453 by
SDS DATA SYSTEMS
Pomona, Calif.

for Goddard Space Flight Center

NATIONAL AERONAUTICS AND SPACE ADMINISTRATION

For sale by the Clearinghouse for Federal Scientific and Technical Information
Springfield, Virginia 22151 – CFSTI price $3.00

Abstract

A study has been performed of ion sources having a magnetically aligned electron beam and which are compatible with a previously designed quadrupole mass spectrometer for planetary atmospheric analysis.

A primary objective was to use the rigid alignment of the electron beam to minimize electron bombardment of the ion source surfaces thereby removing one of the obstacles to stable, long-term operation. A second objective was to formulate the relationships of size, pressure, electron current and applied potentials for a simple model of a magnetic ion source in order to scale the dimensions and pressure over wide ranges. It is shown that for several reasons, size should be scaled down as the operating pressure is increased. For a given system pumping speed, the output current range of the source may be held constant as these two variables are cooperatively changed. The output current can also be set to increase with higher pressure and smaller size. In this process, the pressure and ion current become eventually limited by space charge and ion collisional effects.

Using derived scaling factors a crossed magnetic field ion source was designed for operation at 10^{-1} torr internal pressure. A model, having an internal volume of 4.7×10^{-3} cubic centimeters and tunnel apertures of 0.0025 centimeter diameter was constructed and subjected to test. While such sizes could be feasible for future micro-miniature sources, the construction problems and limited test results indicated that any present operational requirements should be directed toward larger sizes.

TABLE OF CONTENTS

LIST OF SYMBOLS

I_F^+	=	Total ion current formed (amperes)
$I_{T\ max}^+$	=	Total ion current transmitted (amperes)
$I_{sc\ max}^{+\ tun}$	=	Space charge limit of ion current transmitted through a tunnel aperture (amperes)
J^+	=	Ion current density (amperes/meter^2)
P_s	=	Ion source maximum pressure (torr)
P_a	=	Analyzer maximum pressure (torr)
R	=	Radius of ion exit aperture (meters)
L_1	=	Length of ion exit aperture (meters)
w	=	Width of electron entrance aperture (meters)
t	=	Height of electron entrance aperture (meters)
L_2	=	Length of electron entrance aperture (meters)
d	=	Distance from repeller to accelerator (meters)
ad	=	Distance from ionizing plane to accelerator (meters)
ℓ	=	Length of ionizing region from electron entrance aperture to anode (meters)
W	=	Width of ionizing region (meters)
t'	=	Thickness of electron beam (meters)
L	=	Length of electron beam path (meters)
J^-	=	Electron current density (amperes/meter^2)
I^-	=	Ionizing electron current (amperes)
C_1	=	Ion exit aperture gas conductance (liters/second)
α	=	Correction factor for length to diameter ratio for ion exit aperture (dimension-less)
C_2	=	Electron entrance aperture gas conductance (liters/second)
K	=	Correction factor for length to height ratio for electron entrance aperture (dimension-less)

C_s = Ion source gas conductance (liters/second)

Q = Net gas flow (torr-liters/second)

S_a = Speed of pumping system in the analyzer region (liters/second)

D = Differential pumping ratio (dimension-less)

P_c = Critical pressure (torr)

S = Probability of ionization $\left[I_F^+ \text{ (amperes)}/I^- \text{ (amperes)}\right.$ torr-meter of electron path length]

V_r = Potential between repeller and accelerator (volts)

m_e = Mass of electron (kilograms)

M = Mass of positive ion (kilograms)

V_{el} = Energy of ionizing electrons (volts)

x = Ratio of ion source pressure to critical pressure (dimension-less)

i_v = Ratio of ionizing electron current to potential between repeller and accelerator (microamperes/volt)

I^-_{max} = Space charge limit of electron current transmittable through an aperture (amperes)

V_{EA} = Potential of the electron entrance aperture (volts)

V_{FIL} = Potential of the filament from which the electrons are emitted (volts)

ΔV_{min} = $(V_{EA}-V_{FIL})$, electron energy upon reaching the electron entrance aperture (volts)

E_r = Electric field gradient between repeller and accelerator (volts/meter)

B_z = Axial magnetic field along the electron beam (webers/meter^2)

v_e = Velocity of electron beam through the ionizing region (meters/second)

LIST OF SYMBOLS (Continued)

θ	=	Walking angle of electron beam in E_r X B_z field (°)
ΔV_{ion}	=	Ion energy spread (volts)
q	=	Electronic charge (coulombs)
ϕ	=	Ion beam deflection angle due to magnetic (B_z) field (°)
B_y	=	Transverse magnetic field, normal to both E_r and B_z fields (webers/meters^2)
ϕ'	=	Ion beam deflection angle due to magnetic (B_y) field (°)
δ	=	Mass deflection due to axial magnetic field, B_z (meters)
δ'	=	Mass deflection due to transverse magnetic field, B_y (meters)
I_o^-	=	Electron current entering ionizing region (amperes)
λ	=	Mean free path of the gas molecules (meters)
λe	=	Mean free path of the electrons in the gas sample (meters)
λi	=	Mean free path of the ions (meters)
β	=	Length of ion path giving a defined percentage transmission of the ion beam (meters)
N_o	=	Number of ions formed which are transmittable in the absence of gas collision
N	=	Number of ions transmitted of those formed
τ	=	Time constant of ion source (seconds)
V_s	=	Volume of ion source (meter^3)

MAGNETIC ION SOURCE STUDY

INTRODUCTION

One of the primary considerations for the design of a mass spectrometer is the ion source, since both the ion current intensity and conditions are determined here. The ion source imposes all of the initial conditions on the ion beam, which must be within defined limits in order to satisfy the requirements of the mass resolving section of the analyzer. In addition, the confidence in output data from a mass spectrometer can be projected directly to the reliability associated with the ion source, if the system is not continuously calibrated, as is the case in most space-flight systems.

The task of this study was to perform a theoretical investigation of a magnetic ion source capable of approaching pressures in the ionization region of 1×10^{-1} torr and to design and test this source. Other source characteristics desired were improved stability and sensitivity as well as an interchangibility with the existing non-magnetic ion source used in the Specialized Mass Spectrometer Number 2a built under Contract NAS5-3453.

The considerations of concern in the investigation of the magnetic ion source are as follows:

1. Ionization system.
2. Ion source sensitivity.
3. Differential pumping and gas conductance.

4. Internal volume.

5. Ion source time response.

6. Ion source stability with time.

7. Free paths of the electrons and ions.

8. Electron space charge.

9. Ion space charge.

10. Ion source linearity with pressure.

11. Ion energy distribution.

12. Magnetic Mass discrimination.

13. Ion focusing.

14. Compatibility with Specialized Mass Spectrometer Number 2a.

INTERFACE INVARIANTS

The invariants of the ion source, from which the investigation and design proceeded, will now be reviewed. Of the preceding considerations, the invariants include the ionization system and the ion focusing.

The first consideration is the ionization system. The techniques which have been used include thermal ionization, vacuum spark, gas discharge, photo-ionization, ion bombardment, field ionization, and electron bombardment. All these methods are amply reviewed by McDowell.[1] The most common method applied to

1. McDowell, Charles A., Mass Spectrometry, McGraw Hill New York, 1963, pp. 69-103

mass spectrometry is the electron bombardment method since it can produce highly-stable ion beams of relatively high intensities and low-energy spreads. The other methods of ionization are found to be unacceptable due to a low ionization cross section (or in the case of the gas discharge, lack of control), so that the electron bombardment ionization system is the only type of ion source considered for analysis.

An electron beam can be generated by the following types of emitters:

1. Oxide-coated cathodes.
2. Matrix or diffusion cathodes.
3. Refractory-coated cathodes.
4. Thoriated cathodes.
5. Thin film emitters.
6. Tunnel emitters.
7. Cold cathodes.
8. Metal cathodes.
9. Indirectly heated cathodes.

Of these techniques, the most widely used are the hot-wire filament types, since high emission densities and thin electron beams can be obtained. This allows for good focusing of the beam, which creates high electron densities in the ionizing region while keeping the energy spread of the ion beam to a minimum.

This study is based upon electron bombardment ionization using a hot-filament emission system. However, the mechanisms by which

the electron beam is introduced to the ionization chamber vary greatly throughout the field and their characteristics are independent of the variables within the ionizing region. Consequently, this region is treated as an invariant through the course of the study program.

The ion focusing system can be accomplished by either of two means, image focusing or thermal-energy focusing. In an image system, an image of the ionization pattern of the electron beam is produced at the exit slit of the source. This characteristic may be described by Abbe's Law.[2,3] A thermal energy focusing system focuses the ion beam to a crossover point at the exit aperture of the source and is described by Liousville theorem.[4]

The ion source sensitivity is dependent upon the ion source temperature in a thermal system, thus changing the focal point of the source, which can change the ititial conditions of the ions into the analyzer. In systems where tight tolerances have been applied to the initial conditions of the ions, it has been necessary to limit the aberrations by geometrical means, such as baffling. Such is the case in the ion focusing system of the Specialized Mass Spectrometer Number 2a, where a thermal focusing system is used. The ion focusing system will consequently be treated as an invariant in the source investigation and is assumed to be adjustable as an interface mechanism by which the ionizing region characteristics are transformed to a set of analyzer initial conditions.

2. Klemperer, O., Electron Optics, Cambridge University Press, Cambridge, England, 1953, pp. 12-14.

3. Spangenburg, K. R., Vacuum Tubes, McGraw-Hill, New York, 1948 p. 741.

4. Pierce, J. R., Theory and Design of Electron Beams, Van Nostrand, Princeton, N.J., 1954, pp. 48-51.

The ionizing region of the source is the focal point of interest for this study. It encompasses the volume in which the ionization occurs, the necessary ion extraction electrodes, and the interfacing apertures through which the electron beam enters, and through which the ion beam exits.

IONIZING REGION PARAMETERS

Sample Pressure and Flow

The objective of this section is to obtain a set of inter-relationships of the design parameters. To accomplish this task, a model of the ionizing region is set up in Figure 1. It is desirable to obtain these variables as families of curves plotted versus the ion source pressure, since this is the particular parameter of interest for increased design capability.

The ion current formed within the ionizing region can be expressed by the equation

$$I_F^+ = S J^- P_s wt\ell \qquad (1)$$

converting this to current density for a thin sheet of electrons,

$$J^+ = S J^- P_s wt\ell/w\ell$$

or

$$J^+ = S J^- P_s t \qquad (2)$$

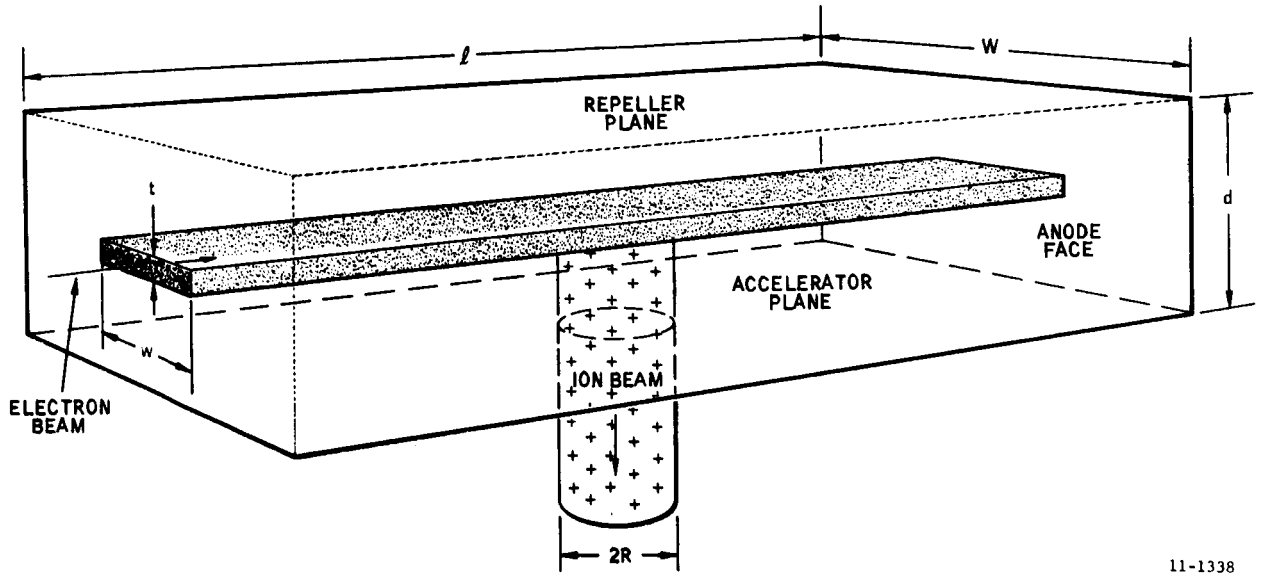
ℓ
W
REPELLER
PLANE
t
d
ANODE
FACE
ACCELERATOR
PLANE
w
ELECTRON
BEAM
ION BEAM
2R
11-1338

FIGURE 1

Assuming a circular aperture for the exit of the ions from the ionization region, this can be expressed in terms of the ion current transmitted, such that

$$I^{+}_{T_{max}} = \pi S J^{-} P_s t R^2 \qquad (3)$$

If the electron current density is held constant, it is seen that the transmitted ion current is only dependent upon the ion source pressure, and two dimensions. However, the ion source pressure can be eliminated by using Guthrie's [5] relationships for the molecular conductance of a short pipe, which state that,

$$C_1 = \frac{\pi}{3}\left[\left(\frac{kT}{2\pi m}\right)^{\frac{1}{2}} \frac{(2R)^3}{L_1}\right]\alpha$$

where

k = Boltzman's constant
T = gas temperature (absolute)
m = molecular mass

For air at 20°C., and with R and L in centimeters,

$$C_1 = 12.1 \quad (2R)^2 \quad \left(\frac{2R}{L_1}\right) \alpha \text{ (liters/second)} \qquad (4)$$

It is now assumed that the total gas conductance out of the ionizing region can be expressed in terms of the flow through two apertures,

5. Guthrie, A., and Wakerling, R.K., Vacuum Equipment and Techniques, McGraw Hill, New York, 1949, pp. 29-47

(1) an annulus for the ion exit, and (2) a thin rectangular tube for the electron entrance.

Guthrie gives the conductance for thin rectangular tube with air at 20°C as

$$C_2 = 30.9 \text{ wt } \left(\frac{t}{L_2}\right) K \quad \text{(liters/second)}$$

where w, t, and L_2 are expressed in centimeters. The values for α are tabulated in Table 1, and those for K are listed in Table 2.

Table 1.

$L_1/2R$	α (determined)	α (calculated)
0.05	0.036	0.036
0.08	0.055	0.056
0.1	0.068	0.070
0.2	0.13	0.13
0.4	0.21	0.23
0.6	0.28	0.31
0.8	0.30	0.38
1.0	0.38	0.43
2.	0.54	0.60
4	0.70	0.75
6	0.77	0.82
8	0.81	0.86
10	0.84	0.88
20	0.91	0.94
40	0.95	0.97

Table 1. (Continued)

$L_1/2R$	α (determined)	α(calculated)
60	0.97	0.98
80	0.98	0.98
100	1	1

Table 2.

L_2/t	0.1	0.2	0.4	0.8	1	2	3	4	5	10
K	0.036	0.068	0.13	0.22	0.26	0.40	0.52	0.60	0.67	0.94

L_2/t	>10
K	$\ln\frac{3}{8}\left(\frac{L_2}{t}\right)$

For simplification, and since the dimensional variation is the same, it is assumed at this point that the conductances are equal and the gas flow is divided equally between the two apertures. This assumption may be re-examined later. Converting to MKS units being used (as defined in the list of symbols), and equating C_1 and C_2, it is seen that

$$wt = 1.57R^2 \left(\frac{\alpha}{K}\right)\left(\frac{2R}{L_1}\right)\left(\frac{L_2}{t}\right) \text{ (meters}^2\text{)} \qquad (5)$$

This expression gives the area of the electron entrance aperture in terms of the square of the ion exit aperture radius, since the other

terms in the expression are constants chosen from the tables. Using the above definition of equal flow through the two apertures, the ion source conductance can be expressed as

$$C_s = 2C_1$$

or

$$C_s = 96.8 \times 10^4 R^2 \left(\frac{2R}{L_1}\right)\alpha \quad \text{(liters/second)} \tag{6}$$

The conductance, C_s, is also related to Q and P.

Thus,

$$C_s = \frac{Q}{P_s - P_a}$$

Where Q = net gas flow, and for this case, is equal to the product of the analyzer pressure and the speed at the pumping system at the analyzer region;

$$Q = S_a P_a \ .$$

Substituting for Q and rearranging the terms,

$$\frac{P_a}{P_a} = 1 + \frac{S_a}{C_s} \ , \tag{7}$$

where the differential pumping ratio, D, is now defined as

$$D = \frac{P_s}{P_a} \tag{8}$$

Solving equation (7) for P_s,

$$P_s = P_a \left(1 + \frac{S_a}{C_s}\right)$$

or, from equation (6),

$$P_s = P_a \left[1 + \frac{S_a}{96.8X10^4 R^2 \alpha} \left(\frac{L_1}{2R}\right)\right] \tag{9}$$

For large differential pumping ratios,

$$\frac{S_a}{C_s} >> 1,$$

and letting

$$\frac{L_1}{R} = K_1$$

it can be written that

$$R = \left(\frac{K_1 P_a S_a}{193.6X10^4 \alpha}\right)^{\frac{1}{2}} P_s^{-1/2} \tag{10}$$

Space Charge in the Ionizing Region

The preceding considerations, however, do not include the effects of space charge within the ionizing region, due to the presence of the electron beam, and ion formation. Let it be assumed that a limited non-linearity can be tolerated in the output current of the source at the maximum pressure.

Brubaker [6] defines the critical pressure in the source as

$$P_c = \frac{3}{4dS}\left(\frac{V_r m_e}{aV_{el}M}\right)^{\frac{1}{2}}$$

and since from his work

$$x = \frac{P_s}{P_c}, \text{ and } i_v = \left(\frac{J^- wt}{V_r}\right)(10^6) \tag{11}$$

then substitution for P_s and J^- in the equation for the transmitted ion current (3) gives

$$I_T^+\Big|_{max} = \left(\frac{3\pi}{4} \times 10^{-6}\right)\left(\frac{m_e}{aV_{el}M}\right)^{\frac{1}{2}} (xi_v)\left(\frac{R}{w}\right)\left(\frac{R}{d}\right) V_r^{3/2} \tag{12}$$

Allowing the width of the electron beam and the distance between the repeller and acelerator to scale directly with the aperture radius

6. Brubaker, W. M., Influence of Space Charge on the Potential Distribution in Mass Spectrometer Ion Sources, J. App. Phys., Vol. 26, No. 8, August 1955

such that

$$\frac{R}{w} = K_2 \quad \text{and} \quad \frac{R}{d} = K_3,$$

then

$$I_T^+\Big|_{max} = \left(\frac{3\pi}{4} \times 10^{-6}\right)\left(\frac{m_e}{aV_{el}M}\right)^{\frac{1}{2}} (xi_v)\, K_2\, K_3\, V_r^{\,3/2} \qquad (14)$$

The values of i_v and x are constants which, to a limited degree can be determined on the basis of the ion current linearity required. Those values are obtained from Brubaker's [6] work as correlated with previous experimental testing.[8]

The effect of flow Q, aperture radius and the other sealed dimensions is implicit in the value of V_r. It is apparent from this that as V_r increases and spacings decrease additional limits will be reached. These are discussed later.

By rewriting equation (11) for the critical pressure, it is seen that

$$P_s = \frac{3x}{4\, dS}\left(\frac{V_r m_e}{aV_{el}M}\right)^{\frac{1}{2}} \qquad (15)$$

8. Robinson, C.F., and Hall, L.G., Small General Purpose Cycloidal-Focusing Mass Spectrometer, Rev. Sci. Inst., Vol 27, No. 7, July 1956

Since $d = \frac{K_3^4}{R}$ and from (10) we can establish R in relationship to gas flow, then

$$P_s = \frac{3K_3x}{4S}\left(\frac{193.6 \times 10^4\alpha}{K_1 P_a S_a}\right)^{\frac{1}{2}} P_s^{\frac{1}{2}} \left(\frac{V_r m_e}{aV_{el}M}\right)^{\frac{1}{2}}$$

or

$$P_s^{\frac{1}{2}} = \frac{3K_3x}{4S}\left(\frac{193.6 \times 10^4\alpha}{K_1 Q}\right)^{\frac{1}{2}} \left(\frac{m_e}{aV_{el}M}\right)^{\frac{1}{2}} V_r^{\frac{1}{2}}$$

Solving for the extraction potential, V_r, gives

$$V_r = \left(\frac{4S}{3K_3x}\right)^2 \left(\frac{aV_{el}M}{m_e}\right) \left(\frac{K_1 Q}{193.6 \times 10^4\alpha}\right) P_s \qquad (16)$$

for large differential pumping ratios.

Consequently, the total ion current transmitted from the source can be written

$$I_T^+\Big|_{max} = \left(\frac{3\pi}{4} \times 10^{-6}\right)\left(\frac{4S}{3K_3x}\right)^3 \left(\frac{K_1 Q}{193.6 \times 10^4\alpha}\right)^{3/2} \left(\frac{aV_{el}M}{m_e}\right)(i_v x)\ (K_2K_3)P_s^{3/2} \qquad (17)$$

which shows that the transmitted ion current increases linearly with the 3/2 power of the ion source pressure when governed by the space charge effects within the ionizing region.

Since the repeller potential, V_r, was shown to increase linearly with the ion source pressure in equation (16), from the relationship

$$i_v = \frac{J^- wt}{V_r} (10^6),$$

and letting

$$\frac{t}{R} = K_4$$

the electron current density may be increased to hold i_v constant and additional ion current as

$$J^- = \frac{i_v K_2 X 10^{-6}}{K_4} \left(\frac{4S}{3K_3 x}\right)^2 \left(\frac{aV_{el}M}{m_e}\right) P_s^2 \qquad (18)$$

Here the electron current density must increase with the square of the ion source pressure.

It is seen that we now have some relatively simple relationships. Extracting only the primary variables

$$R^2 = C_1 Q P_s^{-1}$$

$$V_r = C_2 Q P_s$$

$$J^- = C_3 P_s^2$$

$$I_T^+\Big|_{max} = C_4 V_r^{3/2} = C_5 Q^{3/2} P_s^{3/2}$$

The interpretation of these equations is as follows:

1. With given parameters of electron energy, gas species and relative dimensions of the system it is desired to determine the maximum ion current output as ion source pressure (P_s) is changed.

2. The maximum ion current output is governed by space charge limitations which in turn create non-linearity of ion current transmitted. In certain specific ion sources where non-linearity has been measured as a function of accurately measured ion source pressure and electron current, the results can be placed in the context of Brubaker's "infinite" source equations. By maintaining his relative parameters, (x and i_v), constant and the same relative dimensions, then P_s, J^- and the absolute dimensions may be scaled with no change in the degree of non-linearity.

3. The operating pressure, P_s, is then controlled by the variation of R and the dimensions that are tied to it. V_r can then be increased in proportion to P_s. By the increase in V_r, J^- can also be increased, thereby contributing to improved sensitivity (in spite of the decrease in area for electron and ion transmission).

4. The net result of these changes is an increase in maximum ion current as the ion source shrinks in size and pressure is increased.

5. The gas flow (Q) acceptable by the pumping system also governs the source conductance and the value of R. Consequently, this "independent" control of the area for transmission allows an

increase in ion current. The process of increasing the pumping capacity cannot, however, continue indefinitely, since eventually the ion aperture will exceed the maximum object size acceptable by the analyzer.

The following three conditions which are not imposed upon the source by the preceding equations and which place upper limit restrictions upon the variables thus dealt with are:

1. The maximum ion current which can be passed through the ion exit aperture due to space charge.

2. The maximum electron current which can be transmitted through the electron entrance aperture due to space charge of the beam.

3. The repeller potential approaches the region where voltage breakdown can occur for a corresponding pressure and distance d, because the radius of the apertures are inversely proportional to the square root of the source pressure, and the repeller potential increases linearly with the source pressure.

The maximum ion current which can be passed through an aperture is given by Spangenberg [9] as:

$$I^{+}_{sc}\Big|^{tun}_{max} = .550 \times 10^{-4} V_r^{3/2} \left(\frac{R}{L_1}\right)^2 \left(\frac{m_e}{M}\right)^{\frac{1}{2}} . \qquad (19)$$

(9) Spangenberg, K. R., Vacuum Tubes, McGraw-Hill, New York 1948 pp. 440-448.

Substitution for V_r and R leads to the equation

$$I_{sc}^{+}\Big|_{max}^{tun} = \frac{.550 \times 10^{-4}}{K_1^2}\left(\frac{4S}{3K_3x}\right)^3\left(\frac{aV_{el}M}{m_e}\right)^{3/2}\left(\frac{m_e}{M}\right)^{\frac{1}{2}}\left(\frac{K_1 Q}{193.6 \times 10^4 \alpha}\right)^{3/2} P_s^{3/2} \qquad (20)$$

which shows that the space charge limitation of the maximum ion current which can be passed through an aperture also increases linearly with the 3/2 power of the source pressure.

From (17) and (20) the ratio

$$\frac{I_T^{+}\Big|_{max}}{I_{sc}^{+}\Big|_{max}^{tun}} = \frac{\frac{3\pi}{4} \times 10^{-6} \; (i_v x) \; K_2 K_3}{\frac{5.5 \times 10^{-5}}{K_1^2} \; (aV_{el})^{1/2}} \; ,$$

which, for preliminary values $i_v = 3.8$, $x = .32$, $K_2 = .125$, $K_3 = .925$, $K_1 = 10$, $a = .5$, $V_{el} = 100$ is .102, thus indicating that considerable margin exists to transmit the producable current.

Spangenberg [9] also gives the relationship for the maximum electron current which can be passed through an aperture where a strong axial magnetic field is used to prevent beam spreading. By increasing the current, the potential at the beam center drops below the potential of edge, causing a potential difference which becomes large enough so that the beam is blocked by the space charge. For a beam completely filling the aperture, this effect is reached such when

$$I^-_{max} = 1.025 \left[(V_{EA} - V_{FIL}) \times 10^{-3}\right]^{3/2} \quad (21)$$

where

V_{EA} = potential of the electron accelerator in which the electron entrance aperture is located

V_{FIL} = potential of the filament from which the electrons are emitted.

It is interesting to note that the electron current passing through the aperture is thus independent of the aperture dimensions and solely dependent upon the energy of the electrons, when confined by a magnetic field. This means that the electron current density, J^-, within the ionizing region can be increased without limit by increasing the accelerating potential for the electrons. The minimum accelerating potential can then be found by equating this maximum current with the current necessary to produce the electron current density as required by equation (18). This is found to be

$$\Delta V\Big|_{min} = 9.84 \times 10^{-2} \, (i_v)^{2/3} \left(\frac{4S}{3K_3 x}\right)^{4/3} \left(\frac{aV_{el}M}{m_e}\right)^{2/3} \left(\frac{K_1 Q}{193.6 \times 10^4 \alpha}\right)^{2/3} P_s^{\,2/3} \quad (22)$$

where

$\Delta V = V_{EA} - V_{FIL}$ (the electron energy upon reaching the electron entrance aperture).

The last limitation involves the approach toward voltage breakdown due to decreasing the repeller-accelerator distance, d, while increasing the pressure, P_s, and the repeller potential, V_r. A plot of the voltage breakdown at low pressures is given in Figure 2. It illustrates that the repeller potential must be

$$V_r < V_r\Big|_{max} = f\left[\left(\frac{K_1 Q}{193.6 \times 10^4 \alpha}\right)^{\frac{1}{2}} \qquad \left(\frac{P_s}{K_3}\right)^{\frac{1}{2}}\right] \tag{23}$$

where the function, f, is expressed by the curve in Figure 2.

The maximum pressure to which the ion source will have a linear output is thus dependent only upon a set of constants, since the space charge limitation of the maximum current which can be passed through an aperture imposes an upper limit upon this pressure. Voltage breakdown can also limit this maximum pressure depending upon the scaling factor, K_3, which is chosen. However, the electron current density can easily be obtained to create the necessary ionization by increasing the energy of the electrons at the entrance aperture, but this causes perturbations of the ion extraction field due to the potentials placed upon the side electrodes of the ionization chamber.

A magnetically aligned electron beam passing across an electric field is bent perpendicular orthogonal to the crossed fields. This effect results in a side displacement of the beam, and an increase in the beam thickness due to the cycloidal hopping which creates the side displacement. The sideward displacement of the beam can be expressed by

$$\tan \theta = \frac{E_r}{B_g v_e}$$

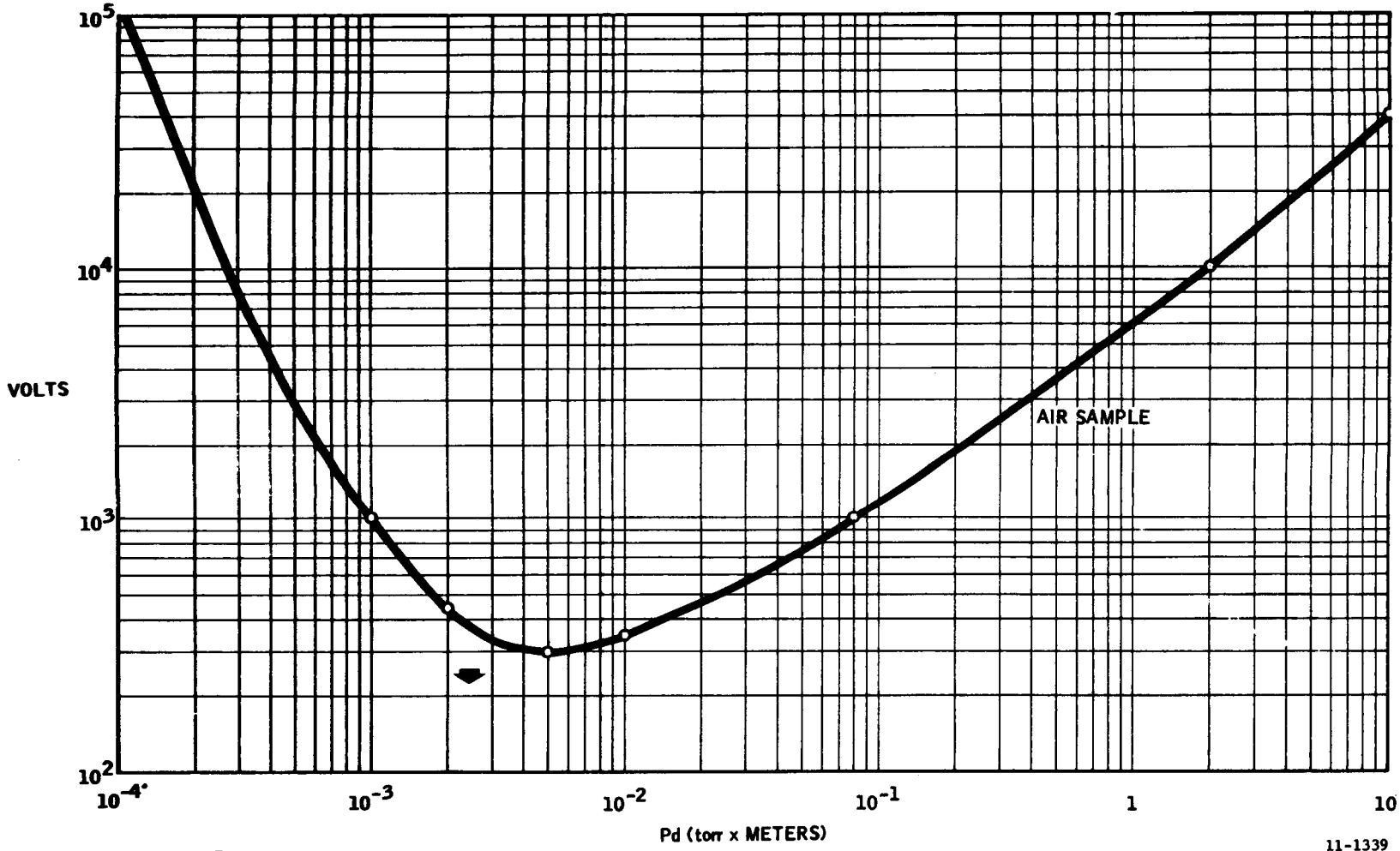

P = PRESSURE (torr)

d = ELECTRODE SPACING (METERS)

FIGURE 2

but E_r is just the repeller potential divided by the distance, d, so that

$$E_r = K_3 \left(\frac{4S}{3K_3 x}\right)^2 \left(\frac{aV_{el}M}{m_e}\right) \left(\frac{K_1 Q}{193.6 \times 10^4 \alpha}\right)^{\frac{1}{2}} P_s^{3/2} \qquad (24)$$

and consequently

$$\tan\theta = \frac{K_3}{v_e B_z} \left(\frac{4S}{3K_3 x}\right)^2 \left(\frac{aV_{el}M}{m_e}\right) \left(\frac{K_1 Q}{193.6 \times 10^4 \alpha}\right)^{\frac{1}{2}} P_s^{3/2} \qquad (25)$$

The thickness of the electron beam is related to the ion energy spread by the relationship

$$\Delta V_{ion} = E_r t'$$

where t' = thickness of the electron beam and t' is calculated as

$$t' = t'\Big|_{max} = \left(t + K_5 \frac{E_r}{B_z^2}\right)$$

where $K_5 = \frac{2m_e}{q}$

Therefore the energy spread of the ion beam is given by

$$\Delta V_{ion} = \left[K_4 \left(\frac{K_1 Q}{193.6 \times 10^4 \alpha} \right)^{\frac{1}{2}} \right.$$

$$\left. + \frac{K_5 K_3}{B_z^2} \left(\frac{4S}{3K_3 x} \right)^2 \left(\frac{aV_{el} M}{m_e} \right) \left(\frac{K_1 Q}{193.6 \times 10^4 \alpha} \right)^{\frac{1}{2}} P_s^{\,2} \right]$$

$$\times \left[K_3 \left(\frac{4S}{3K_3 x} \right)^2 \left(\frac{aV_{el} M}{m_e} \right) \left(\frac{K_1 Q}{193.6 \times 10^4 \alpha} \right)^{\frac{1}{2}} P_s \right] \qquad (26)$$

This shows that when P_s is very very small, the ion energy spread increases, approximately linearly with the ion source pressure, however, when P_s becomes relatively large, the spread then increases with the cube of the pressure. However, it is apparent that the stronger that the magnetic field is, the shorter is the cycloidal hop height, and the closer the beam thickness approaches the height, t, of the electron entrance aperture.

A magnetic field, used to align and constrain the ionizing electron beam, also creates mass discriminating deflections of the ion beam generated by the source, and the amount of the deflection occurring is mass dependent, i.e., the deflections are proportional to the molecular weight of the ion species. Referring to Figure 3 for the system coordinates, the force equations are such that

$$M\ddot{x} = \dot{y}\, q\, B_z$$

$$M\ddot{y} = q\, E_r - \dot{x}\, q\, B_z$$

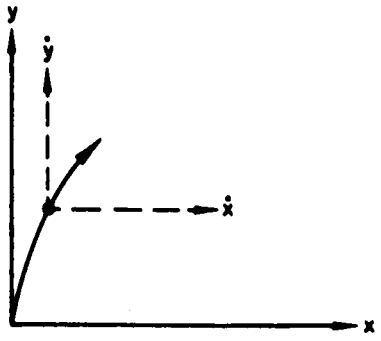

Figure 3.

It is then assumed that x is negligible in the short paths that are considered of interest. Thus, integration gives

$$M\dot{x} = y\, q\, B_z \tag{27}$$

$$M\dot{y} = q\, E_r\, t + M\dot{y}_o \quad (t \text{ is time in sec}) \tag{28}$$

These equations then give the x and y directional velocities as a function of time. Integrating again on $\dot{y}$ gives the y directional position as

$$M\, y = \frac{q\, E_r\, t^2}{2} + M\, \dot{y}_o\, t + M\, y_o \tag{29}$$

However, the initial velocity, $\dot{y}_o$, and the initial position, y_o, are assumed to be zero, so that the ion beam deflection angle, ϕ, can be written as

$$\tan\, \phi = \frac{\dot{x}}{\dot{y}} = \frac{y\, B_z}{E_r\, t} \tag{30}$$

Solving equation (29) for the time, t, and substituting into equation (30) gives the expression

$$\tan \phi = B_z \left(\frac{qy}{2 M E_r} \right)^{\frac{1}{2}} \tag{31}$$

The distance, y, however, is approximately equal to one half the distance from the repeller to the first slit

$$y_{max} \approx ad \tag{32}$$

Substituting for y and E_r show that the angle ϕ is

$$\tan \phi \Big|_{max} = \left(\frac{qB_z^2}{2M} \right)^{\frac{1}{2}} \left(\frac{a}{K_3^2} \right)^{\frac{1}{2}} \left(\frac{3K_3 x}{4S} \right) \left(\frac{m_e}{aV_{el}M} \right)^{\frac{1}{2}} P_s^{-1} \tag{33}$$

The angle ϕ of deflection thus decreases linearly with the ion source pressure. The amount of deflection is given by

$$\delta = \int_o^{\delta} dx$$

However, since tan ϕ = dx/dy, solving equation (31) for dx gives

$$dx = B_z \left(\frac{q}{2M E_r} \right)^{\frac{1}{2}} y^{\frac{1}{2}} \, dy \tag{34}$$

or

$$\delta = B_z \left(\frac{q}{2M E_r} \right)^{\frac{1}{2}} \int_o^y y^{\frac{1}{2}} \, dy$$

$$\delta = \frac{2 B_z}{3} \left(\frac{q}{2M E_r} \right)^{\frac{1}{2}} y^{3/2} \tag{35}$$

Again, substituting for E_r and y gives the expression,

$$\delta = \frac{2}{3} \left(\frac{q B_z^2}{2M} \right)^{\frac{1}{2}} \left(\frac{a^{3/2}}{K_3^2} \right) \left(\frac{3K_3 x}{4S} \right) \left(\frac{m_e}{aV_{el}M} \right)^{\frac{1}{2}} \left(\frac{K_1 Q}{193.6 \times 10^4 \alpha} \right)^{\frac{1}{2}} P_s^{-3/2} \tag{36}$$

Specific Values

The previous equations denote the parameters of importance and their interrelationships using the specified assumptions. These parameters then can be plotted versus pressure for a set of initial scaling factors.

The values obtained are the maximum numbers which optimize the parameters to an ion source maximum pressure. For example, while the maximum ion current transmitted increases with the 3/2 power of the maximum pressure, due to an increase in V_r and J^-, as the source pressure is reduced from the maximum, the ion current transmitted will decrease linearly with the pressure as the other variables are held constant. Choosing a set of scale factors for the aperture radius and length ratio gives

$$K_1 = 10 \text{ and } \alpha = .74$$

For $S_a = 10^{-1}$ liters/sec, and $P_a \Big|_{max} = 10^{-5}$ torr, or

$$Q = 1 \times 10^{-6} \frac{\text{torr-liters}}{\text{sec}}$$

then

$$R = .264 \times 10^{-5} P_s^{-\frac{1}{2}} \text{ meters}$$

$$= 10.39 \times 10^{-5} P_s^{-\frac{1}{2}} \text{ inches}$$

The width of the electron beam, w, is then picked to be 8R so that the beam walking will still allow the centering of the beam over the ion exit aperture.

Thus

$$K_2 = .125$$

Choosing the length to thickness ratio of the electron entrance aperture such that

$$\frac{L_2}{t} = 5$$

then

$$t = .216\ R \quad \text{or } K_4 = .216$$

and letting $d = 5t$

$$d = 1.081\ R \quad \text{or } K_3 = .925$$

The ionizing probability of air is given as

$$S = 10^3 \text{ amps } (I^+)/\text{amp } (I^-) \text{ - meter - torr}$$

for electron energies of $V_{el} = 70$ V.

Placing the center of the electron beam at a distance equal to one half the repeller distance sets

$$a = .5,$$

and to obtain a non-linearity of 3% or less corresponds to

$$x = .32 \text{ and } i_v = 3.8$$

For these scaling factors, and choosing a worst case mass of m/e 44, the following relationships are derived:

$$V_r = 398\ P_s \text{ (volts)}$$

$$I_T^+\Big|_{max} = 1.570 \times 10^{-6}\ P_s^{3/2} \text{ (amps)}$$

$$J^-\Big|_{max} = 1.252 \times 10^{8}\ P_s^{2} \text{ (amps/meter}^2\text{)}$$

$$I_{sc}^+\Big|_{\substack{tun \\ max}} = 1.540 \times 10^{-5}\ P_s^{3/2} \text{ (amps)}$$

$$\Delta V_{min} = 12.96\ P_s^{2/3} \text{ (volts)}$$

$$E_{r\ max} = 139.2 \times 10^{6}\ P_s^{3/2} \text{ (volts/meter)}$$

$$\Delta V_{ion} = 79.4\ P_s + 221 \times 10^{3}\ \frac{P_s^{3}}{B_z^{2}} \text{ (volts)}$$

$$\tan \theta = 28.1\ \frac{(P_s)^{3/2}}{B_z}$$

$$\tan \phi\Big|_{max} \text{ (for helium, m/e 4)} = 1.165 \times 10^{-3}\ B_z\ P_s^{-1}$$

$$\delta = 1.106 \times 10^{-9}\ B_z\ P_s^{-3/2} \text{ (for helium, m/e 4) (meters)}$$

These parameters are plotted versus the maximum ion source pressure in Figures 4, 5, 6, 7, and 8.

It must be realized, however, that these curves are valid only for the set of scale factors chosen, and while the slope will not change with the scaling, the absolute values will.

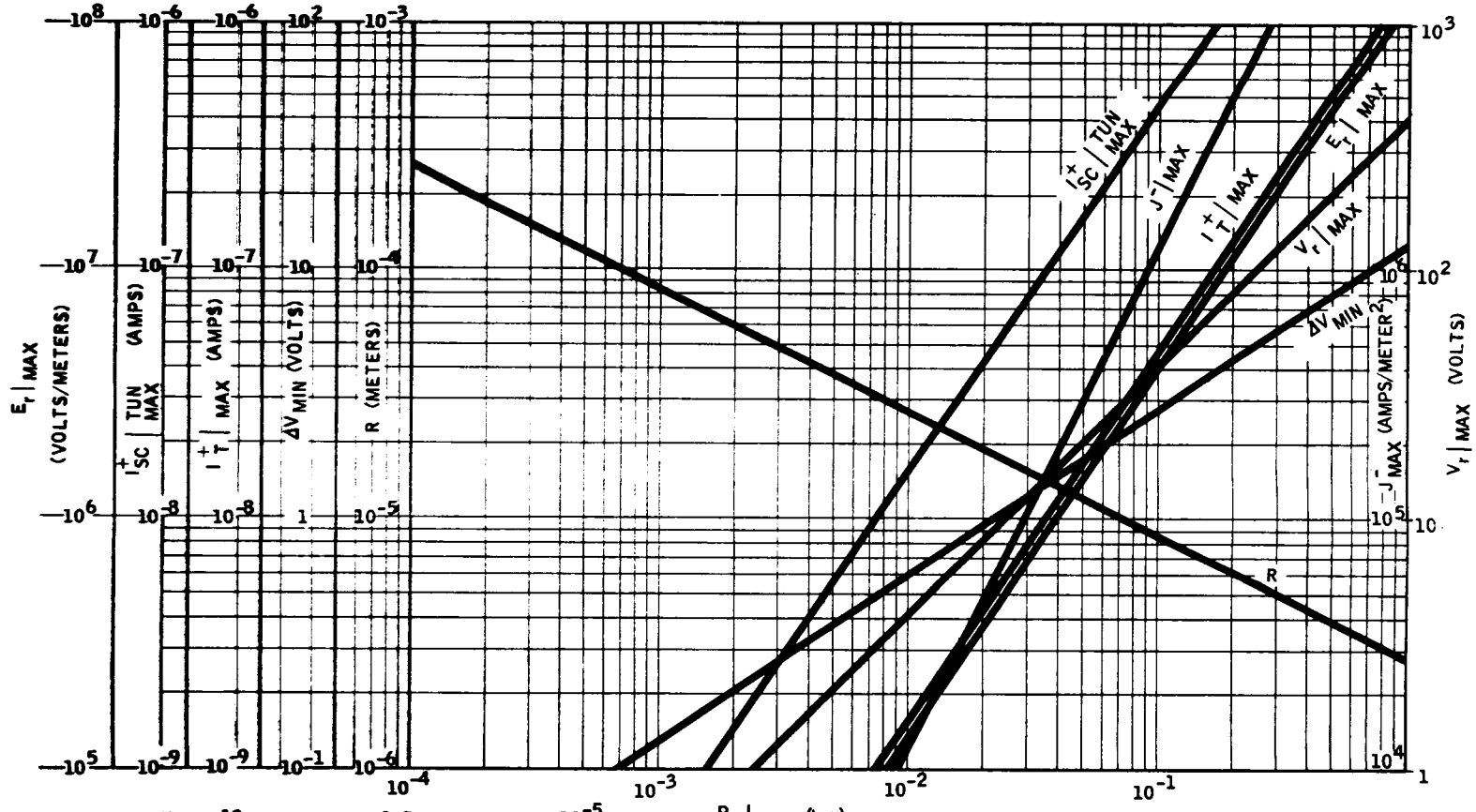

$K_1 = 10$ $\quad a = 0.5$ $\quad P_a|_{max} = 10^{-5}$ torr

$K_2 = .125$ $\quad x = .32$

$K_4 = .216$ $\quad i_v = 3.8$ $\quad S_a = 0.1$ liters/sec

$K_3 = .925$ $\quad m/e = 44$

$V_{el} = 70$ v.

11-1340

FIGURE 4

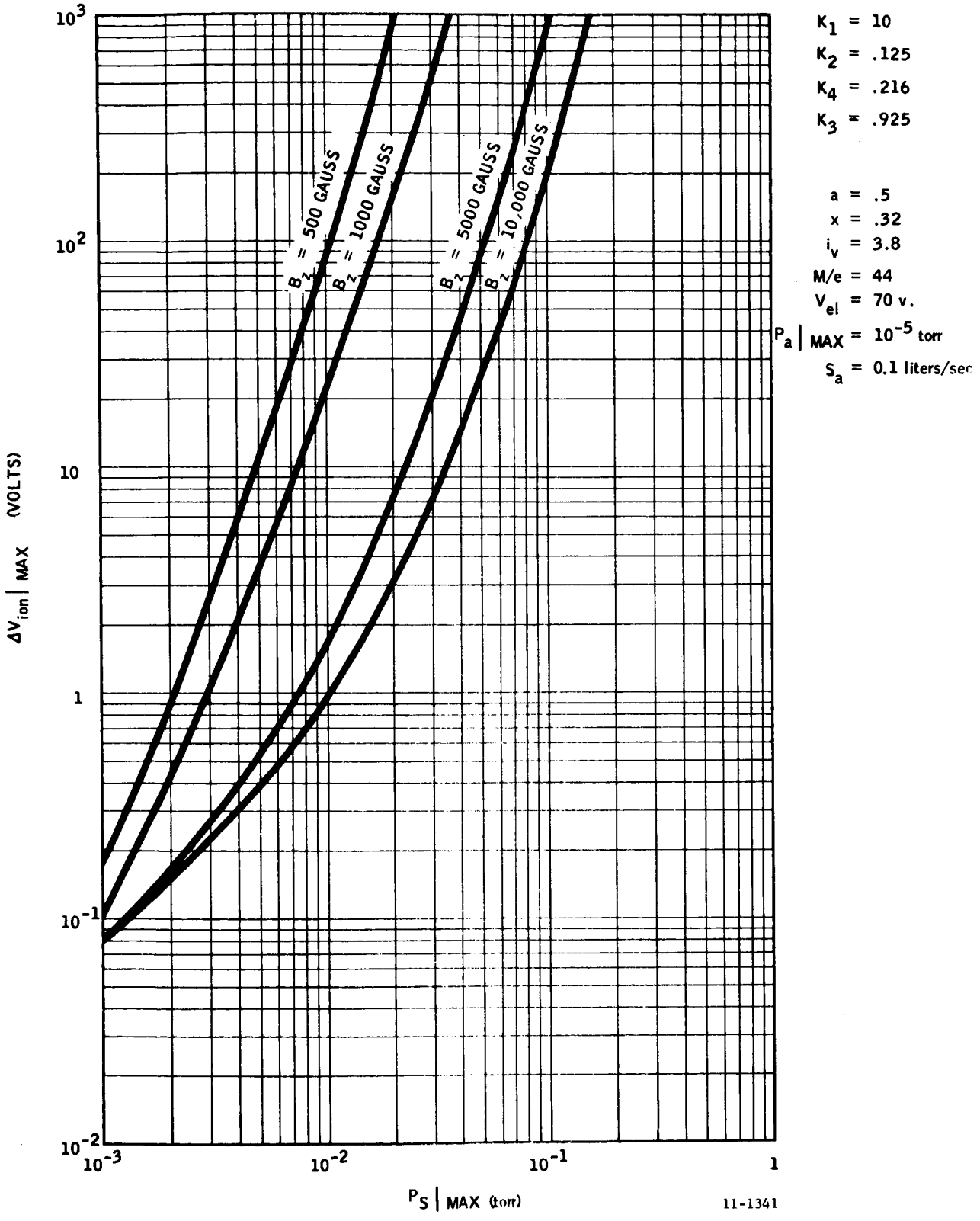
10^3
10^2
10
1
10^{-1}
10^{-2}
10^{-3}
10^{-2}
10^{-1}
1
$\Delta V_{ion} \mid MAX$ (VOLTS)
$P_S \mid MAX$ (torr)
B_z = 500 GAUSS
B_z = 1000 GAUSS
B_z = 5000 GAUSS
B_z = 10,000 GAUSS
K_1 = 10
K_2 = .125
K_4 = .216
K_3 = .925
a = .5
x = .32
i_v = 3.8
M/e = 44
V_{el} = 70 v.
$P_a \mid MAX = 10^{-5}$ torr
S_a = 0.1 liters/sec
11-1341

FIGURE 5

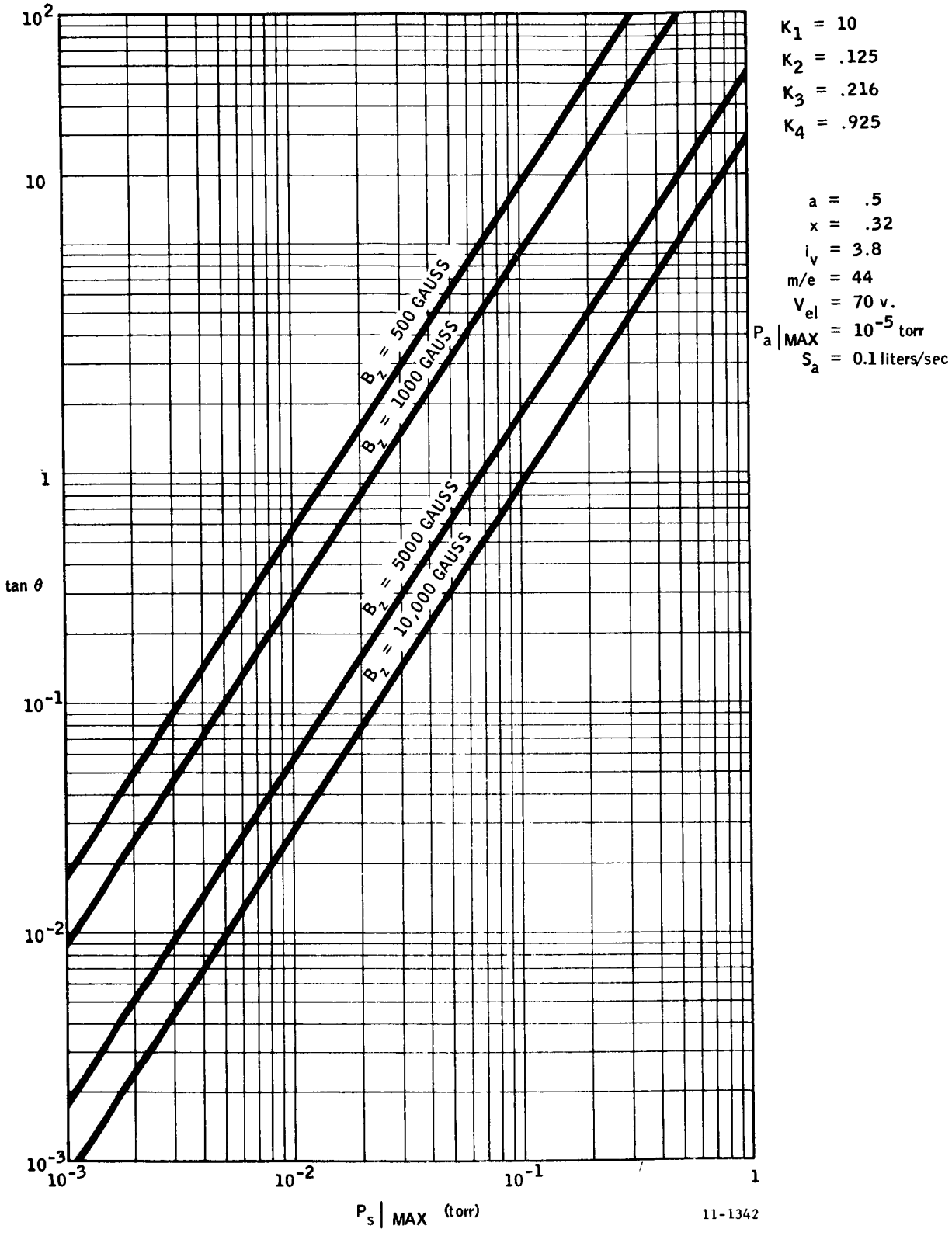
10^2
10
1
10^{-1}
10^{-2}
10^{-3}
tan θ
B_z = 500 GAUSS
B_z = 1000 GAUSS
B_z = 5000 GAUSS
B_z = 10,000 GAUSS
10^{-3}
10^{-2}
10^{-1}
1
$P_s \mid_{MAX}$ (torr)
11-1342
K_1 = 10
K_2 = .125
K_3 = .216
K_4 = .925
a = .5
x = .32
i_v = 3.8
m/e = 44
V_{el} = 70 v.
$P_a \mid_{MAX}$ = 10^{-5} torr
S_a = 0.1 liters/sec

FIGURE 6

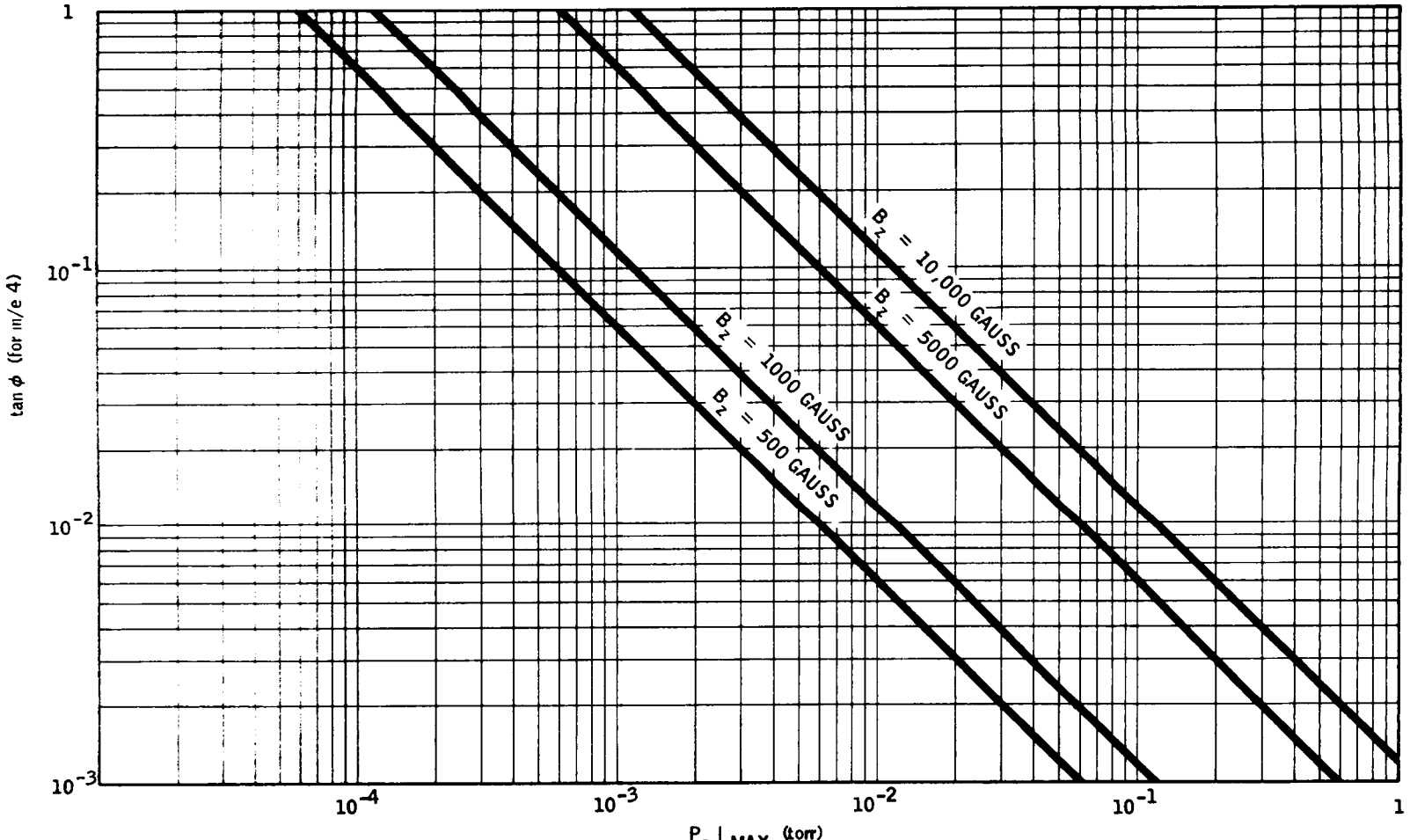

K_1 = 10 a = .5 V_{el} = 70 v.

K_2 = .125 x = .32 P_a | MAX = 10^{-5} torr

K_4 = .216 γ = 3.8 S_a = 0.1 liters/sec

K_3 = .925 π/e = 4

11-1343

FIGURE 7

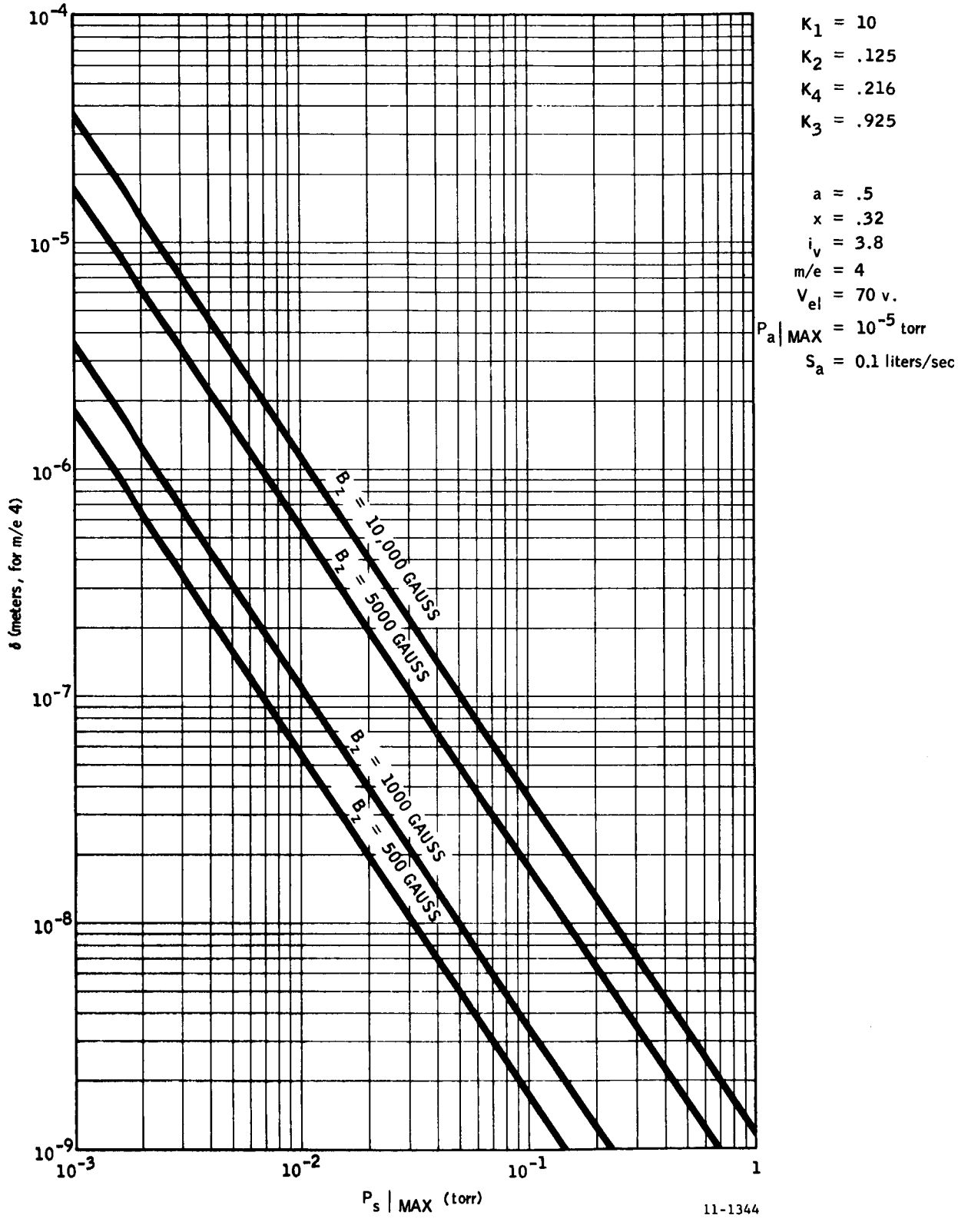
10^{-4}
10^{-5}
10^{-6}
10^{-7}
10^{-8}
10^{-9}
10^{-3}
10^{-2}
10^{-1}
1
B_z = 10,000 GAUSS
B_z = 5000 GAUSS
B_z = 1000 GAUSS
B_z = 500 GAUSS
ϕ (meters, for m/e 4)
P_s | MAX (torr)
11-1344
K_1 = 10
K_2 = .125
K_4 = .216
K_3 = .925
a = .5
x = .32
i_v = 3.8
m/e = 4
V_{el} = 70 v.
P_a | MAX = 10^{-5} torr
S_a = 0.1 liters/sec

FIGURE 8

Gas Collision Limits

For a designed value of maximum ion source pressure, an electron current density, J^-, is then specified. The mean free path of the electrons can be expressed by

$$\lambda_e = 4\,(2)^{\frac{1}{2}}\,\lambda \tag{37}$$

where λ is the mean free path of the gas molecules. For an air sample,

$$\lambda = \frac{4.86 \times 10^{-5}}{P_s} \text{ (meters)} \tag{38}$$

$$\text{and } \lambda_e = 27.5 \times 10^{-5}/P_s \text{ (meters)} \tag{39}$$

Both λ_e and λ are plotted in Figure 9.

It is desirable in most ion sources to fix the electron current density by keeping the electron current passing through the ionizing region constant. In order to obtain regulation, it must then be necessary to keep the collision probability of the electrons to a minimum. Assuming a collision probability of 1%, from Lambert's law,

$$\frac{I^-}{I_o} = e^{-L/\lambda_e} = .99$$

$$\text{or} \qquad L = \frac{2.74 \times 10^{-6}}{P_s} \text{ (meters)} \tag{40}$$

where L is the length of the electron path required to obtain 99% transmission of the electron beam.

L is also plotted versus the maximum ion source pressure in Figure 9. From this curve, it becomes apparent that for high pressures in the source, regulation of the electron current by collection in the ionizing region implies very short electron path lengths, and consequently very short ionizing regions. Another governing factor which follows from this discussion is the path length of the ions formed at the high pressure levels. Again reverting to Lambert's law, it is seen that

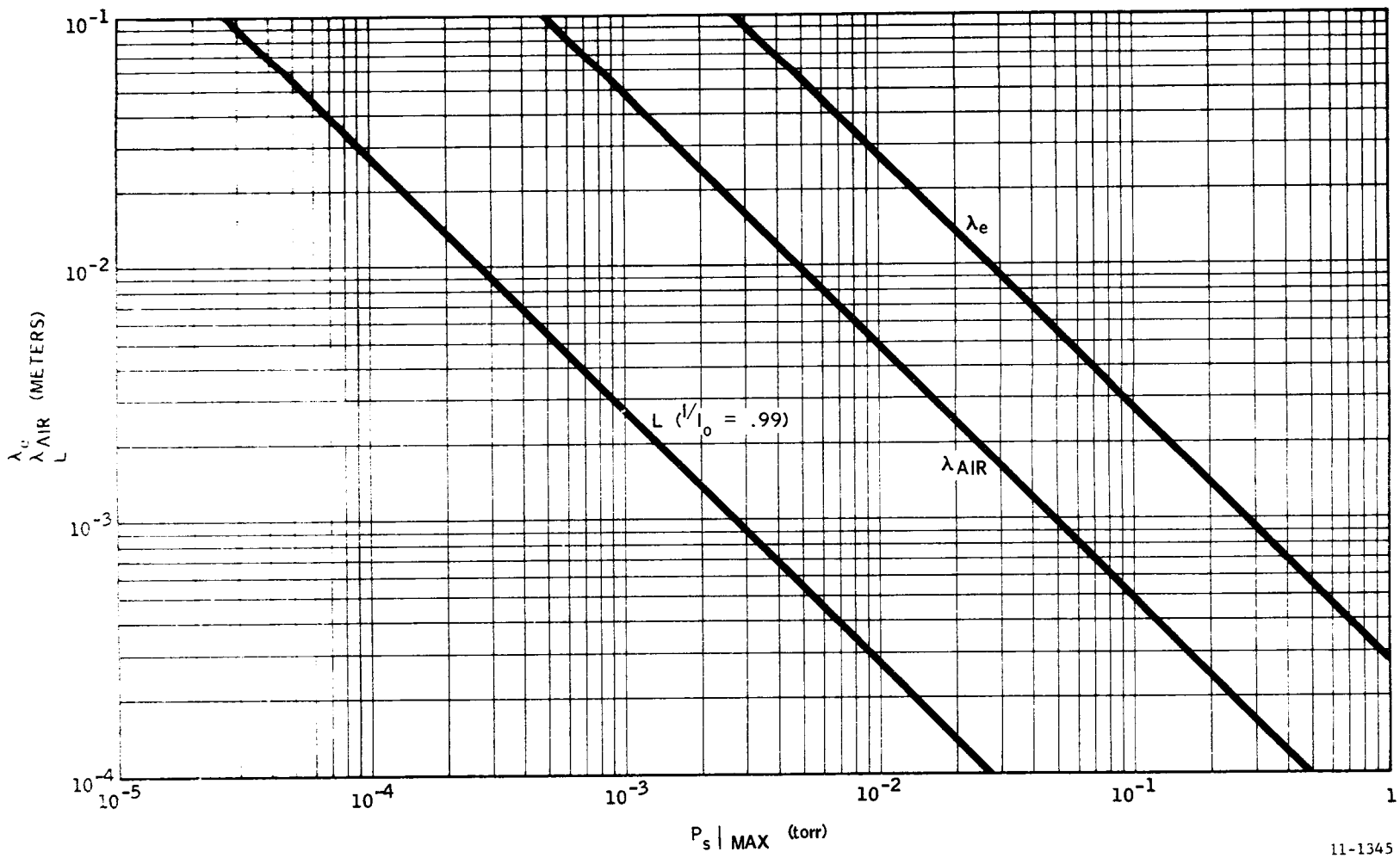
10^{-1}
10^{-2}
10^{-3}
10^{-4}
λ_e
λ_{AIR}
L (I/I_o = .99)
λ_e λ_{AIR} L (METERS)
10^{-5}
10^{-4}
10^{-3}
10^{-2}
10^{-1}
1
P_s | MAX (torr)
11-1345

FIGURE 9

$$N = N_o e^{-\beta/\lambda_i}$$

where

N_o = number of ions formed

N = number of ions transmitted

β = path length of the ion

λ_i = mean free path of the ion

Again, for 99% transmission of the ions formed

$$\frac{N}{N_o} = e^{-\beta/\lambda_i} = .99$$

The mean free path of ions is given by

$$\lambda_i = (2)^{\frac{1}{2}} \lambda$$

or for air, $\lambda_i = \frac{6.87 \times 10^{-5}}{P_s}$ (meters) (41)

Consequently it is then seen that

$$\beta = \frac{6.84 \times 10^{-7}}{P_s} \text{ (meters)} \quad (42)$$

These two variables are plotted versus the maximum ion source pressure in Figure 10.

This curve shows that for high pressures within the ionizing region, the path length for the ions to travel through the high pressure region must become extremely short. Otherwise the output ion current will vary with the pressure not only due to the ions formed in the electron beam, but also due to the change in the path length, β, of the ion beam lowering the percentage of ions capable of being transmitted.

Design of the Test Model

Using the relationships derived in the foregoing section, a test model of a magnetic ion source capable of pressures up to 10^{-1} torr was evaluated. From a manufacturing viewpoint, size limitations are placed upon the source, however, from the curves, an idea of the relative sizes of the parameters can be obtained.

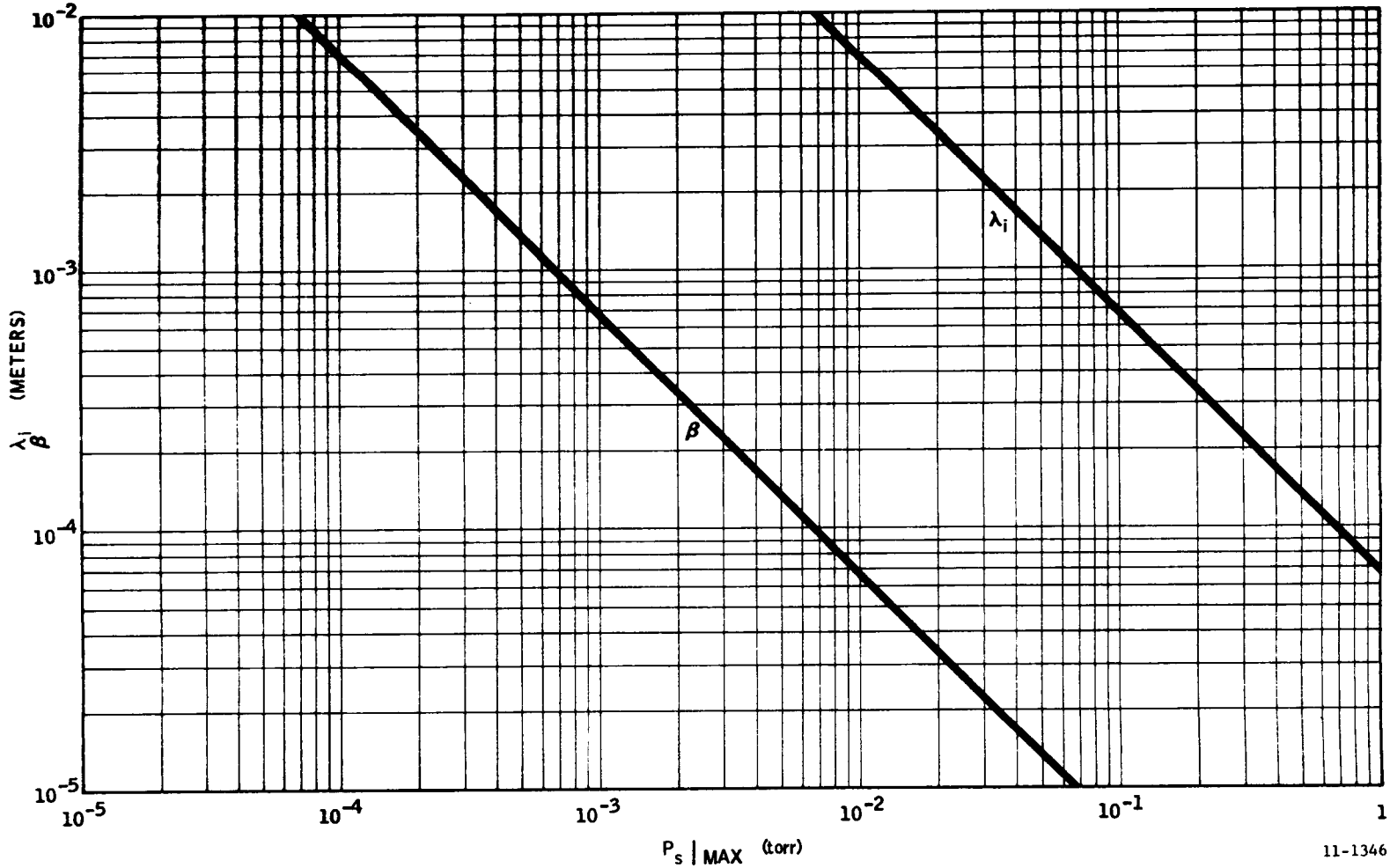
10^{-2}
10^{-3}
10^{-4}
10^{-5}
λ_i
β
λ_i β (METERS)
10^{-5}
10^{-4}
10^{-3}
10^{-2}
10^{-1}
1
P_s | MAX (torr)
11-1346

FIGURE 10

Thus, from the figures for a $P_s\big|_{max} = 10^{-1}$ torr, with the constants for scaling assumed, the following parameters are given:

$$R = 8.35 \times 10^{-6} \text{ meters}$$

$$V_r\big|_{max} = 38.9 \text{ volts}$$

$$J^-\big|_{max} = 1.25 \times 10^{6} \text{ amps/cm}^2$$

$$I_T^+\big|_{max} = 6.8 \times 10^{-8} \text{ amps}$$

$$I_{sc}^+\Big|_{max}^{tun} = 6.8 \times 10^{-7} \text{ amps}$$

$$\Delta V_{min} = 2.8 \text{ volts}$$

$$E_r = 4.4 \times 10^{6} \text{ amps/meter}^2$$

$$\Delta V_{ion} = 228.94 \text{ volts } (B_z = 10{,}000 \text{ gauss})$$
$$= 891.9 \text{ volts } (B_z = 5{,}000 \text{ gauss})$$
$$= 22108 \text{ volts } (B_z = 1{,}000 \text{ gauss})$$
$$= 88408 \text{ volts } (B_z = 500 \text{ gauss})$$

$$\tan\theta = .898 \ (B_z = 10{,}000 \text{ gauss})$$
$$= 1.78 \ (B_z = 5{,}000 \text{ gauss})$$
$$= 8.98 \ (B_z = 1{,}000 \text{ gauss})$$
$$= 17.8 \ (B_z = 500 \text{ gauss})$$

$$\tan\phi\big|_{max} = .012 \ (B_z = 10{,}000 \text{ gauss})$$
$$= .006 (B_z = 5{,}000 \text{ gauss})$$
$$= .0012 (B_z = 1{,}000 \text{ gauss})$$
$$= .0006 (B_z = 500 \text{ gauss})$$

Flow Time Constant

The time constant, τ, associated with an ion source is defined by the expression

$$\tau = V_s/C_s$$

or

$$\tau = \frac{V_s P_s}{P_a S_a} = \frac{V_s P_s}{Q}$$

But it is seen that the volume can be written as

$$V_s = \ell W d$$

Assuming the width of the source to be four times the width of the electron entrance aperture, and for 99% transmission of the electron beam

$$\ell \leq L,$$

then the volume is expressed by

$$V_s = \left(\frac{10.96 \times 10^{-6}}{K_2 K_3}\right)\left(\frac{K_1 Q}{193.6 \times 10^4 \alpha}\right) P_s^{-2}$$

The time constant is then shown to be

$$\tau = \left(\frac{1}{Q}\right)\left(\frac{10.96 \times 10^{-6}}{K_2 K_3}\right)\left(\frac{K_1 Q}{193.6 \times 10^4 \alpha}\right) P_s^{-1}$$

$$\delta = 3.5 \times 10^{-8} \text{ meters} \quad (B_z = 10{,}000 \text{ gauss})$$

$$= 1.75 \times 10^{-8} \text{ meters} \quad (B_z = 5{,}000 \text{ gauss})$$

$$= 3.5 \times 10^{-9} \text{ meters} \quad (B_z = 1{,}000 \text{ gauss})$$

$$= 1.75 \times 10^{-9} \text{ meters} \quad (B_z = 500 \text{ gauss})$$

$$\lambda_e = 2.75 \times 10^{-3} \text{ meters}$$

$$\lambda_{air} = 4.86 \times 10^{-4} \text{ meters}$$

$$L = 2.74 \times 10^{-5} \text{ meters (for 99\% transmission)}$$

$$\lambda_i = 6.87 \times 10^{-4} \text{ meters}$$

$$\beta = 6.84 \times 10^{-6} \text{ meters (for 99\% transmission)}$$

From the scaling factors, the dimensions of the source are then calculated to be

$$t = 1.80 \times 10^{-6} \text{ meters}$$

$$w = 6.68 \times 10^{-5} \text{ meters}$$

$$L_1 = 8.35 \times 10^{-5} \text{ meters}$$

$$L_2 = 9.01 \times 10^{-6} \text{ meters}$$

$$d = 9.03 \times 10^{-6} \text{ meters}$$

$$ad = 4.52 \times 10^{-6} \text{ meters}$$

The length of the ionizing region should be no longer than the required path length to obtain the transmission of the electron beam, or

$$\ell \leq L = 2.74 \times 10^{-5} \text{ meters}$$

which then gives a time constant of

$$\tau = .0066 \text{ second}$$

It is clear that for the theoretical basis of the design, the one parameter which is unrealizable is the creation of the extremely high energy spreads of the ions at high pressures. It is possible, however, to eleiminate the cycloidal hopping of the electron beam and the walking angle ϕ, by the use of a cross magnetic field applied only in the region of crossed E field. Reverting back to the equations for the electron motion (27) and (28), the magnetic field can then be expressed by

$$B = jB_y + kB_z \tag{43}$$

and thus

$$\ddot{x} = \left(\frac{qB_z}{m_e}\right) \dot{y} - \left(\frac{qB_y}{m_e}\right) \dot{z} + \left(\frac{q}{m_e}\right) E_r$$

$$\ddot{y} = -\left(\frac{qB_z}{m_e}\right) \dot{x}$$

$$\ddot{z} = \left(\frac{qB_y}{m_e}\right) \dot{x}$$

Making the substitutions

$$\omega_z = \frac{qB_z}{m_e}, \quad \text{and } \omega_y = \frac{qB_y}{m_e},$$

and integration gives

$$\dot{y} = -\omega_z x + \dot{y}_o$$

$$\dot{z} = \omega_y x + \dot{z}_o$$

where $\dot{x}_o$ and $\dot{y}_o$ are the initial velocities along the respective axes. Substituting to find the x-axis acceleration gives

$$\ddot{x} = -\omega_z^2 x + \omega_z \dot{y}_o - \omega_y^2 x - \omega_y \dot{z}_o + \frac{q}{m_e} E_r$$

$$= -x(\omega_y^2 + \omega_z^2) + \frac{q}{m_e} E_r + \omega_z \dot{y}_o - \omega_y \dot{z}_o$$

The solution to this differential equation is given by

$$x = \left[x_o - \left(\frac{q}{m_e} E_r + \omega_z \dot{y}_o - \omega_y \dot{z}_o \right) / \omega^2 \right] \cos \omega t$$

$$+ \left(\frac{\dot{x}_o}{\omega} \right) \sin \omega t + \left(\frac{q}{m_e} E_r + \omega_z \dot{y}_o - \omega_y \dot{z}_o \right) / \omega^2 \qquad (43)$$

The y and z directional velocities are then

$$\dot{y} = -\omega_z \left[x_o + \left(\frac{q}{m_e} E_r + \omega_z y_o - \omega_y z_o \right) / \omega^2 \right] \cos \omega t$$

$$- \left(\frac{\dot{x}_o \omega_z}{\omega} \right) \sin \omega t - \left(\frac{q}{m_e} E_r + \omega_z \dot{y}_o - \omega_y \dot{z}_o \right) \omega_z / \omega^2 + \dot{y} \qquad (44)$$

$$\dot{z} = \omega_y \left[x_o - \left(\frac{q}{m_e} E_r + \omega_z \dot{y}_o - \omega_y \dot{z}_o \right) / \omega^2 \right] \cos \omega t$$

$$+ \left(\frac{\dot{x}_o \omega_y}{\omega} \right) \sin \omega t + \frac{q}{m_e} E_r + \omega_z \dot{y}_o - \omega_y \dot{z}_o \Big) \omega_y / {}^2 + \dot{z}_o \qquad (45)$$

where the substitution has been made that

$$\omega^2 = \left(\omega_y^2 + \omega_z^2 \right)$$

If a cross magnetic field is used, the effects of the extraction field, E_r, can be reduced by setting.

$$\frac{q}{m_e} E_r - \omega_y \dot{z}_o = o$$

where

$$\dot{z}_o = \left(\frac{2q V_{el}}{m_e} \right)^{\frac{1}{2}}$$

The B_y field is thus

$$B_y = \frac{E_r}{z_o} \qquad (47)$$

and the equations of motion become

$$x = \left(x_o - \frac{\omega_y \dot{y}_o}{\omega^2}\right) \cos\omega t + \left(\frac{\dot{x}_o}{\omega}\right) \sin\omega t + \frac{\omega_z \dot{y}_o}{\omega^2} \tag{48}$$

$$\dot{y} = \omega_z \left(x_o - \frac{\omega_y \dot{y}_o}{\omega^2}\right) \cos\omega t - \left(\frac{\dot{x}_o \omega_z}{\omega}\right) \sin\omega t - \frac{\omega_z^2 \dot{y}_o}{\omega^2} + \dot{y}_o \tag{49}$$

$$\dot{z} = \omega_y \left(x_o - \frac{\omega_z \dot{y}_o}{\omega^2}\right) \cos\omega t + \left(\frac{\dot{x}_o \omega_y}{\omega}\right) \sin\omega t + \frac{\omega_z \omega_y \dot{y}_o}{\omega^2} + \dot{z}_o \tag{50}$$

This shows that utilization of a cross magnetic field, B_y, will accomplish a balancing force against the electrostatic ion extraction field which will eliminate the cycloidal hopping of the electron beam. With this field, the ion energy spread, ΔV_{ion}, reduces to

$$\Delta V_{ion} = E_r t \tag{51}$$

and the walking angle, θ, is reduced to zero. However, there will exist some y-directional electron beam spreading due to the initial velocity along this axis, which cannot be avoided. Evaluating the ion energy spread with the cross magnetic field gives

$$\Delta V_{ion} = K_4 K_3 \left(\frac{4S}{3K_3 x}\right)^2 \left(\frac{aV_{el} M}{m_e}\right) \left(\frac{K_1 Q}{193.6 \times 10^4}\right) P_s \tag{52}$$

and thus at 10^{-1} torr using the scaling factors,

$$\Delta V_{ion} = 79.5 P_s$$

$$= 7.95 \text{ volts}$$

For the scaling factors previously used, if a cross magnetic field is desired, it is seen that

$$B_y = K_3 \left(\frac{m_e}{2qV_{el}}\right)^{1/2} \left(\frac{4S}{3K_3 x}\right)^2 \left(\frac{aV_{el} M}{m_e}\right) \left(\frac{K_1 Q}{193.6 \times 10^4}\right)^{1/2} P_s^{3/2}$$

or

$$B_y = 28.0\ P_s^{3/2}$$

At 10^{-1} torr, this then becomes

$$B_y = .885 \text{ webers/meter}^2$$
$$= 8850 \text{ gauss}$$

This field will also contribute a discriminating deflection upon the mass to charge ratios formed within the source, giving a discriminating angle ϕ' and a deflection δ'. At 10^{-1} torr, these are

$$\tan \phi' = 1.165 \times 10^{-3}\ B_y\ P_s^{-1}$$
$$= 1.031 \times 10^{-2} \text{ (for helium, m/e 4)}$$

and δ'
$$= 1.106 \times 10^{-9}\ B_y\ P_s^{-3/2}$$
$$= 3.10 \times 10^{-8} \text{ meters (for helium, m/e 4)}$$

These additional and modified parameters for the use of the cross magnetic field are plotted versus $P_s|_{max}$ in Figure 11.

The practicality of manufacturing an ion source to such small dimensions thus becomes the limiting factor for building the test model, and especially obtaining the requirements for the flow restricting apertures. At the time it was decided to use two identical circular apertures for both the ion exit and electron entrance to reduce the complexity of such small pieces. This does, however, create more of a strain upon the alignment within the ionizing region in order to keep the electron beam directly above the ion exit aperture. While the conductances of the two apertures remain equal, upon which the foregoing equations were developed, the scaling factors must necessarily be changed. Consequently,

$$t = 2R \text{ or } K_4 = 2$$

$$w = 2R \text{ or } K_2 = 5$$

The aperture length to diameter ratio was picked at 5, for manufacturing purposes, and thus the aperture dimensions can be specified from equation (10) for the following assumed constants:

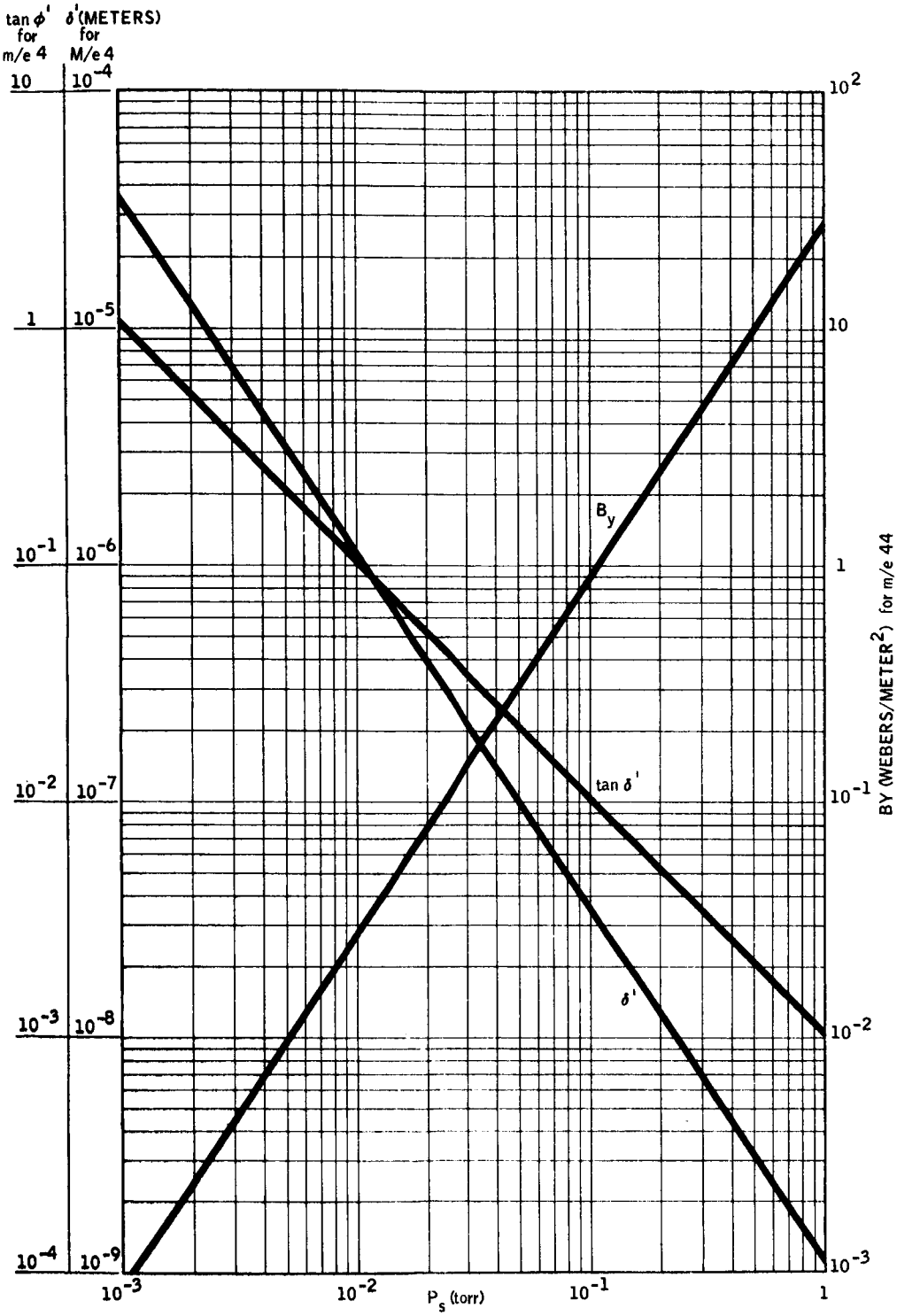

$K_1 = 10$ a = 0.5 $P_a|_{MAX} = 10^{-5}$ torr

$K_2 = .125$ x = .32 $S_a = 0.1$ liters/sec

$K_4 = .216$ $i_v = 3.8$

$K_3 = .925$ $V_{el} = 70$ v

11-134

FIGURE 11

$$P_a\big|_{max} = 1 \times 10^{-5} \text{ torr}$$

$$S_a = 0.1 \text{ liters/sec}$$

Thus,

$$K_1 = 10$$

$$R = 8.35 \times 10^{-6} \text{ meters}$$

or $$R = 3.28 \times 10^{-4} \text{ inches}$$

and $$L = 8.35 \times 10^{-5} \text{ meters}$$

or $$L = 3.28 \times 10^{-3} \text{ inches}$$

For construction, the lower manufacturing limits which were obtainable from an outside source, were

$$R = 5.0 \times 10^{-4} \text{ inches}$$

$$L = 5.0 \times 10^{-3} \text{ inches}$$

This meant that either the upper source pressure limit must be reduced, or the analyzer pressure allowed to increase. The analyzer pressure was then allowed to increase, giving

$$P_a\big|_{max} = 2.31 \times 10^{-5} \text{ torr}$$

for $S_a = 0.1$ liters/sec , $K_1 = 10$, and $P_s\big|_{max} = 10^{-1}$ torr. From these values, the remaining dimensions can be set forth.

In order to obtain a scaling factor for the repeller - accelerator distance, d, it is necessary to examine the mean free path of the ions formed. It is then seen that to obtain 99% of the transmittable ions formed in the electron beam through the accelerator aperture that the distance from the beam to the accelerator, ad, must be

$$ad \leq \beta = 6.84 \times 10^{-6} \text{ meters}$$

$$= 2.69 \times 10^{-4} \text{ inches}$$

Thus, assuming the ionizing electron beam to be placed midway between the repeller and accelerator, or a = .5, then the distance d is found as

$$d \leq 2\beta = 1.368 \times 10^{-5} \text{ meters}$$
$$= 5.38 \times 10^{-4} \text{ inches}$$

Under these conditions, for the aperture size assumptions, it is seen that the electron beam must be thicker than the height through which it must pass. Thus for the two equal sized apertures, to allow the 5/d ratio to decrease, it is seen that an appreciable loss of ion current will take place due to a decrease in the transmittable ion current formed. In the test model produced, the distance, d, was set at .015 inches, which corresponds to an ad = .0075 inches, and at 10^{-1} torr gives

$$\frac{N}{N_o} = 75.8\%$$

The ion current output versus the ion source pressure for a $P_s|_{max} = 10^{-1}$ torr will look as illustrated in Figure 12. This curve shows the non-linearity in the ion source output caused by an increase in the collision frequency of the ions with the gas due to the shortening of the ion mean free path with pressure, for a constant β equal to .0075 inch.

It was also decided that regulation of the ionizing electron current be controlled by the total emission, thus not having the necessity of shortening the length of the ionizing region to such extremely short spacings in the test model. As designed, the maximum path length, L, of the electrons was set at .075 inches. The electron transmission at 10^{-1} torr is then calculated to be

$$\frac{I}{I_o} = 50.0\%$$

and the electron current transmitted to the anode versus ion source pressure for a $P_s|_{max} = 10^{-1}$ torr and L = .075 inches is illustrated in Figure 13.

The scaling factor, K_3, used in the test model was thus

$$K_3 = 3.33 \times 10^{-2}$$

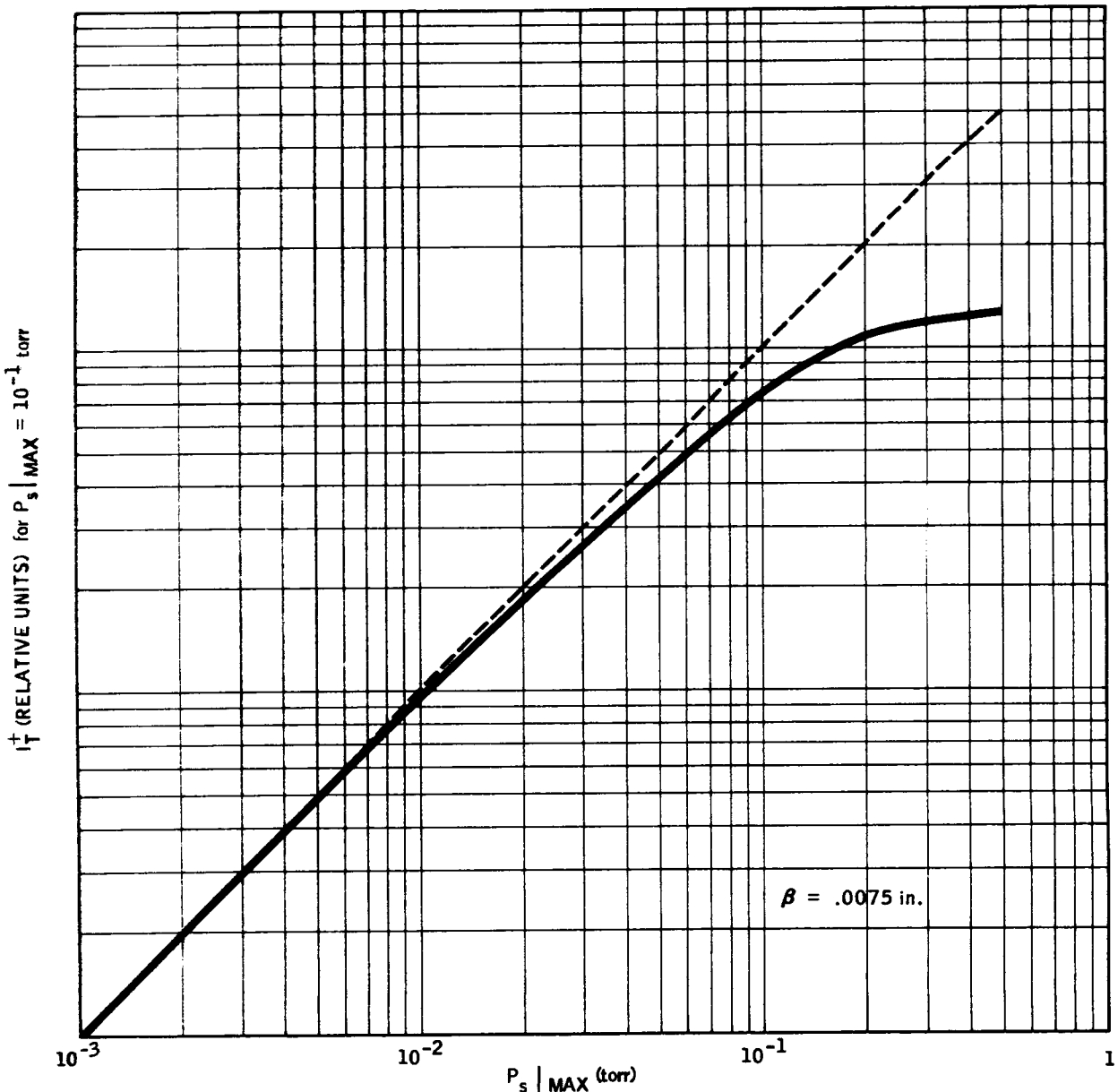

11-1348

FIGURE 12

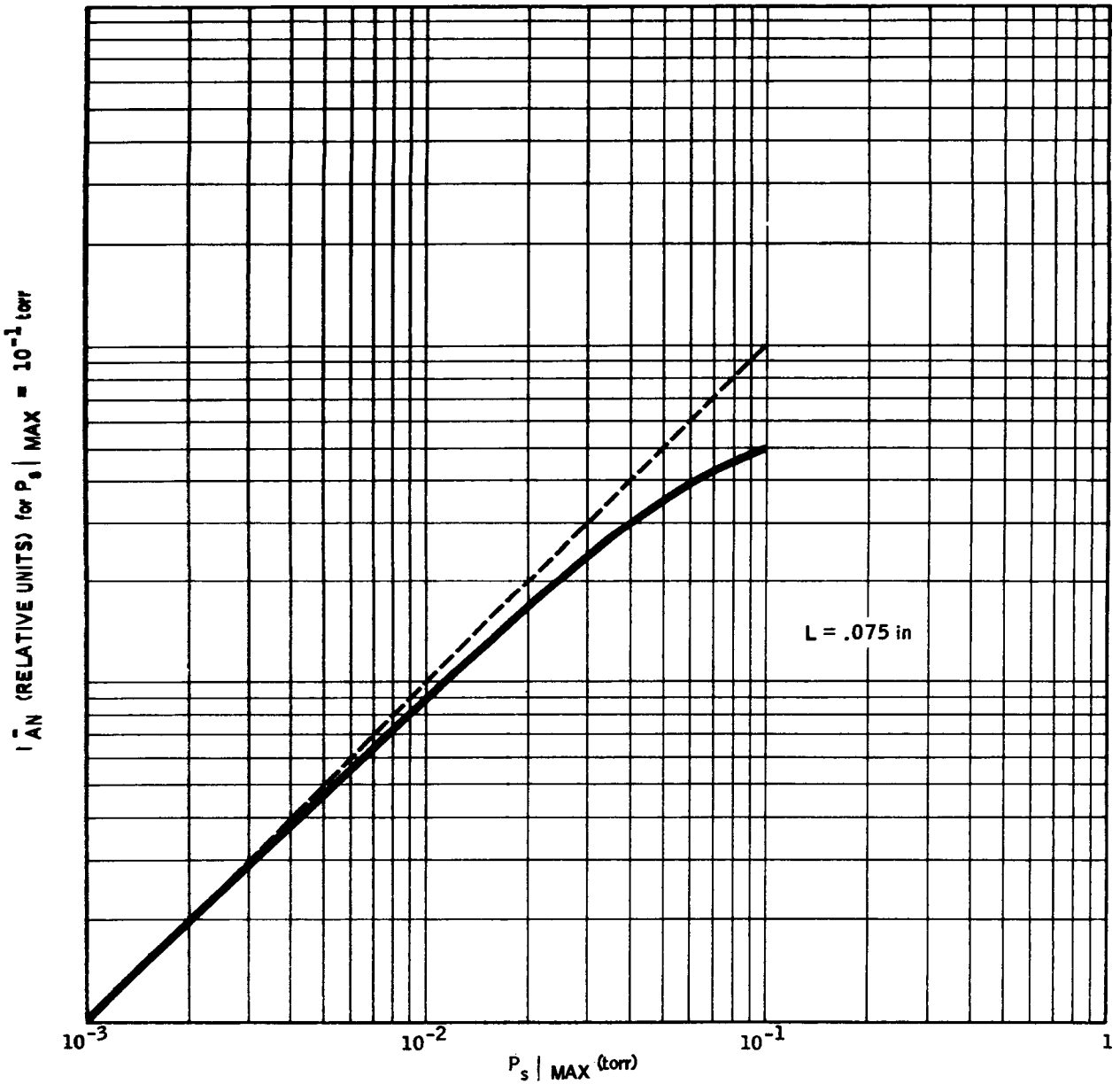

11-1349

FIGURE 13

It must be stated that prior to the writing of this report, many of the interrelations developed in the parameter consideration section had not been accomplished. Due to a personnel change after the hardware had been fabricated, the presented techniques for evaluation were developed. Consequently, the necessary values of the required potentials, currents, etc., were not rigorously worked out, but rather, values for these variables were assumed.

Thus, an associated non-linearity was chosen where $x = 10$, and $i_v = .03$. For these values and scaling factors, the values of the parameters of 10^{-1} torr become

$$V_r = 72.4 \text{ volts}$$

$$I_T^+\Big|_{max} = 4.31 \times 10^{-9} \text{ amps}$$

$$J^- = 5.44 \times 10^{-4} \text{ amps/meter}^2 \text{ and for this case}$$

$$I^- = J^- \pi R^2$$

$$I^- = 2.172 \times 10^{-6} \text{ amps}$$

$$I_{sc}^+\Big|_{\substack{tun \\ max}} = 1.190 \times 10^{-6} \text{ amps}$$

$$\Delta V_{min} = .1713 \text{ volt}$$

$$E_r = 1.90 \times 10^5 \text{ volts/meter}$$

A cross magnetic field was designed to eliminate the electron beam walking angle, and also the increase in the beam thickness due to the cycloidal hopping. Consequently, for $B_z = 4000$ gauss; it is seen that

$$B_y = .03825 \text{ webers/meter}^2 = 382.5 \text{ gauss}$$

$$\tan\theta = 0$$

$$\Delta V_{ion} = 4.825 \text{ volts}$$

$$\tan\phi = 1.456 \quad \text{(for M/e 4)}$$

$$\delta = .742 \times 10^{-9} \text{ meters} \quad \text{(for M/e 4)}$$

$$\tan\phi' = .1391 \quad \text{(for M/e 4)}$$

$$\delta' = 7.08 \times 10^{-11} \text{ meters} \quad \text{(for M/e 4)}$$

At 10^{-1} torr, the ionizing electron current, I^-, necessary to produce the maximum transmittable current is seen to be 2.172×10^{-6} amperes, however the amount reaching the anode of this pressure is 50% of that entering the ionizing region, so that an expected current maximum reaching the anode would be

$$I^-_{an} = 1.086 \times 10^{-6} \text{ amperes}$$

and the transmitted ion current would be 75.8% of the transmittable ion current formed, or

$$I^+_{out}\Big|_{max} = 3.27 \times 10^{-9} \text{ amperes}$$

The ion source as designed had an internal volume capacity of the ionizing region of 4.67×10^{-3} cc, not including the inlet sample line to the source. The gas conductance out of source is 23.1×10^{-3} cc/sec so that the time constant of the source is calculated to be

$$\tau = 202 \text{ milliseconds}$$

The magnetic ion source was designed, as shown in Figure 14. The primary purpose in this design was to attempt to realize the above parameters and to keep the size of the source within the dimensions of the specialized Mass Spectrometer Number 2a. Measurements of the magnetic fields of both the axial and cross magnetic fields were attempted with a Hall effect probe having an active area of .030 inch by .060 inch. This probe was too large to make accurate measurements, however, rough estimates indicated that the axial field was about 4000 gauss, with the transverse field being approximately 100 gauss.

The unit was assembled (see Figure 14) and placed in an ion source testing fixture which had a sample inlet system attached to the inlet tube leading to the ionization chamber.

TEST RESULTS

The testing of the magnetic ion source was set up in a three-phase program, in the following order:

1. Electron gun tuneup

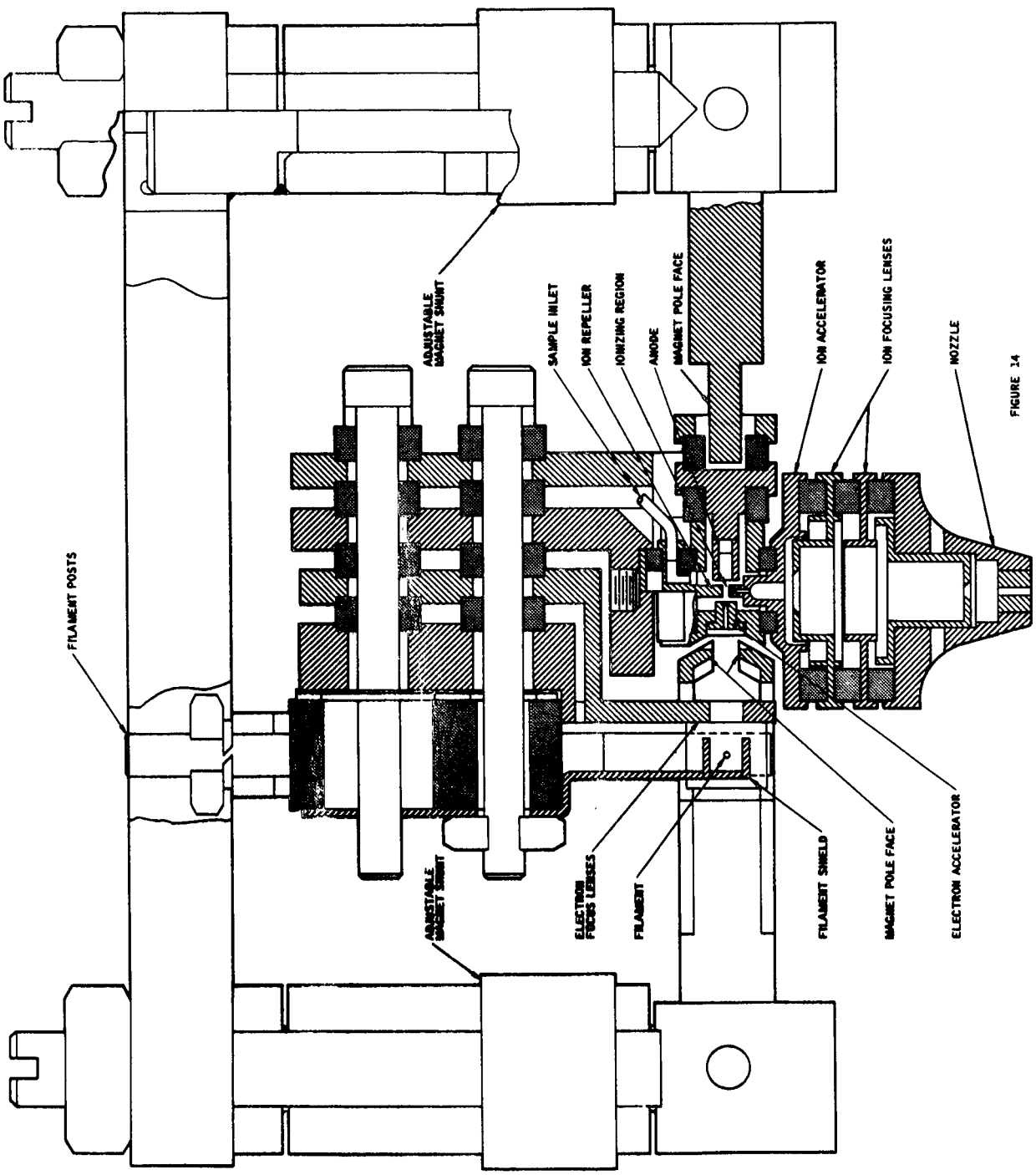
FILAMENT POSTS
ADJUSTABLE MAGNET SHUNT
SAMPLE INLET
ION REPELLER
IONIZING REGION
ANODE
MAGNET POLE FACE
ION ACCELERATOR
ION FOCUSING LENSES
NOZZLE
ADJUSTABLE MAGNET SHUNT
ELECTRON FOCUS LENSES
FILAMENT
FILAMENT SHIELD
MAGNET POLE FACE
ELECTRON ACCELERATOR

FIGURE 14

2. Ion Current tuneup

3. Parameter and characteristic testing.

The initial electron focusing in the electron gun and ionizing region appeared to have a relatively high output of ion current for what appeared to be a correct amount of electron current on the anode in the ionization chamber. However, it was noted that neither the repeller, accelerator or ion focus electrodes had any effect upon the ion output, which remained constant without regard to the potentials applied to these electrodes. The only change observed in this ion current appeared when the sample pressure was changed. This indicated that the ion current was being formed outside the ionizing region, and most probably in the electron gun area, with the ions being formed from the background gas inside the vacuum system. To eliminate this problem, a cylindrical can was placed around the source, with the exception of the nozzle aperture, in order to shield the collector from any ions produced from the background gas. Further testing with the shield in place eliminated this ion current.

With 0.5 microamperes of electron current reaching the anode, no ion current was produced by the ion source having an ionization chamber pressure of 100 microns. The repeller potential affected the anode current, but the ion accelerator had absolutely no effect at all. It was then surmized that the current reaching the anode was following stray magnetic field lines other than through the ionizing region, and yet passing closely to the repeller or wire lead connected to the repeller. This indeed proved to be the case, since after a box shield was placed around the exterior open surface of the anode, no current could reach the anode except by going through the ionizing region. Testing proved that with the shield in place, both the repeller and ion accelerator affected the anode current.

Maximum current to the anode was achieved with the ion accelerator having a more positive potential than the repeller, indicating that the transverse magnets had their polarity reversed. The polarity of the transverse magnets is undefined in the calculation for their field strength, and it was anticipated that they might be reversed. Reversing of the polarity of the cross magnetic field allowed tuning up of the electron gun so that the maximum

electron current collected at the anode was 0.1 microamperes out of a total emission of 200 microamperes.

No ion current was observed on the collector though, and nothing could be done with the ion focus electrodes to obtain any reading on an electrometer set to read currents as low as 10^{-14} amperes. The ion source was then removed, and both the electron accelerator and ion accelerator apertures were inspected under a highpower microscope, revealing that 30% of the electron entrance aperture was plugged with a metallic substance, and the ion exit aperture had no hole at all. The surfaces of both aperture pieces were very non-uniform, and appeared to be burned in several areas. This indicated that electron beam drilling of these very small holes was not a reliable process, and that perhaps other techniques of obtaining holes of these dimensions should be investigated. Limitations of funding, however, concluded the effort required to complete this task, so the project was abandoned at this point.

FUTURE STUDY AREAS

Although the theoretical calculations indicate the feasibility of building a high pressure magnetic ion source capable of handling pressures of 1×10^{-1} torr, it has been found that the manufacturing and fabrication techniques required to build such an instrument were beyond capability for the existing funding. It has been shown, however, that electron focusing through a .001 inch diameter hole can be achieved and that with advanced construction and handling capabilities such an ion source is not beyond the realm of possibility. At present, it is more useful to think of larger aperture sizes for sources not requiring such high pressures, so that very high differential pumping ratios can be avoided.

It has been shown that for a given conductance, and choosing an aperture length to diameter, the gradient, E_r, the ionic energy spread, V_{ion} and the electron current density, J^-, the ion current transmittable, and the effects of a magnetic field are defined by choosing a set of scaling factors.

Figure 15 plots the ion source conductance as a function of the time response of the source for various ionizing region volumes. Thus, for a specified conductance, the necessary volume can be interpolated between the lines in order to satisfy a required system time response.

The necessary calculations having been completed for on source design, it is seen that the remaining considerations depend upon the practical means of obtaining very small apertures and using ultra-clean techniques in order to remove the possibility of filling the apertures with foreign material. These factors have created the major difficulties in the design for a differential pumping ratio of 10^4, however, for ratios of 10^3 or lower, it is felt that the enlarged aperture sizes are within the capability of existing techniques.

ACKNOWLEDGMENT

It is a pleasure to acknowledge Mr. Michael R. Ruecker for the benefit of many helpful discussions dealing with this treatise.

ION SOURCE CONDUCTANCE VERSUS SYSTEM TIME RESPONSE FOR
IONIZING REGION VOLUME DETERMINATION

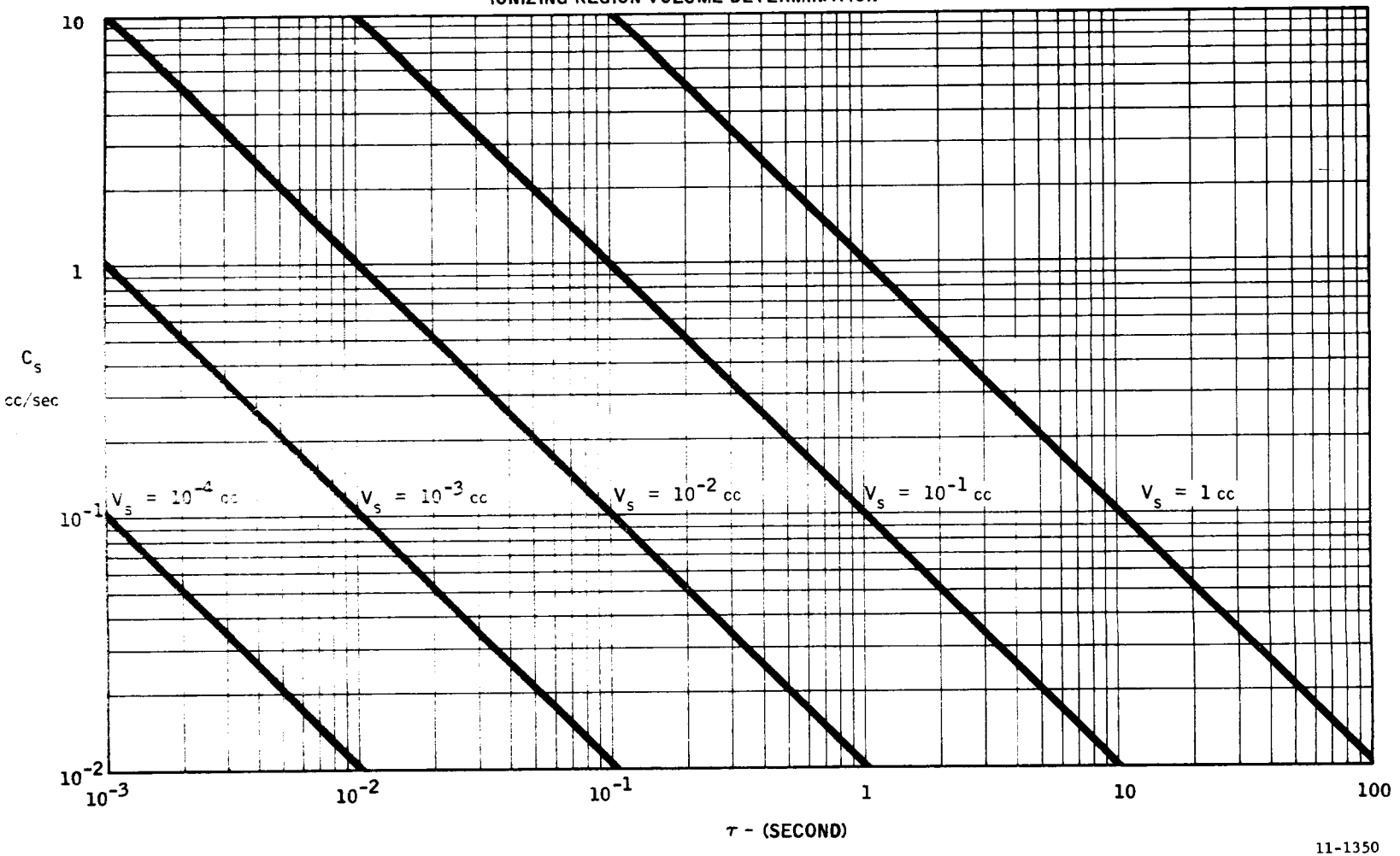

FIGURE 15